Gastroenterology 2022;163:1613–1629

# Context-Dependent Roles of *Hes1* in the Adult Pancreas and Pancreatic Tumor Formation

Saiko Marui,[1] Yoshihiro Nishikawa,[1,2,3] Masahiro Shiokawa,[1] Masataka Yokode,[1] Shimpei Matsumoto,[1] Yuya Muramoto,[1] Sakiko Ota,[1] Takeharu Nakamura,[1] Hiroyuki Yoshida,[1] Hirokazu Okada,[1] Takeshi Kuwada,[1] Tomoaki Matsumori,[1] Katsutoshi Kuriyama,[1] Akihisa Fukuda,[1] Dieter Saur,[4,5] Takashi Aoi,[2] Norimitsu Uza,[1] Yuzo Kodama,[3] Tsutomu Chiba,[6] and Hiroshi Seno[1]

*[1]Department of Gastroenterology and Hepatology, Kyoto University Graduate School of Medicine, Kyoto, Japan; [2]Division of Advanced Medical Science, Graduate School of Science, Technology and Innovation, Kobe University, Kobe, Hyogo, Japan; [3]Department of Gastroenterology, Kobe University Graduate School of Medicine, Kobe, Hyogo, Japan; [4]Department of Internal Medicine II, Klinikum rechts der Isar Technische Universität München, München, Bayern, Germany; [5]Division of Translational Cancer Research, German Cancer Research Center (DKFZ) and German Cancer Consortium (DKTK), Heidelberg, Baden-Württemberg, Germany; and [6]Department of Gastroenterology and Hepatology, Kansai Electric Power Hospital, Osaka, Japan*

**BACKGROUND & AIMS:** The Notch signaling pathway is an important pathway in the adult pancreas and in pancreatic ductal adenocarcinoma (PDAC), with hairy and enhancer of split-1 (HES1) as the core molecule in this pathway. However, the roles of HES1 in the adult pancreas and PDAC formation remain controversial. **METHODS:** We used genetically engineered dual-recombinase mouse models for inducing *Hes1* deletion under various conditions. **RESULTS:** The loss of *Hes1* expression in the adult pancreas did not induce phenotypic alterations. However, regeneration was impaired after caerulein-induced acute pancreatitis. In a pancreatic intraepithelial neoplasia (PanIN) mouse model, PanINs rarely formed when *Hes1* deletion preceded PanIN formation, whereas more PanINs were formed when *Hes1* deletion succeeded PanIN formation. In a PDAC mouse model, PDAC formation was also enhanced by *Hes1* deletion after PanIN/PDAC development; therefore, *Hes1* promotes PanIN initiation but inhibits PanIN/PDAC progression. RNA sequencing and chromatin immunoprecipitation-quantitative polymerase chain reaction revealed that *Hes1* deletion enhanced epithelial-to-mesenchymal transition via *Muc5ac* up-regulation in PDAC progression. The results indicated that HES1 is not required for maintaining the adult pancreas under normal conditions, but is important for regeneration during recovery from pancreatitis; moreover, *Hes1* plays different roles, depending on the tumor condition. **CONCLUSIONS:** Our findings highlight the context-dependent roles of HES1 in the adult pancreas and pancreatic cancer.

*Keywords:* Pancreatic Ductal Adenocarcinoma; PanIN; Muc5ac; Notch.

Pancreatic ductal adenocarcinoma (PDAC) is a lethal malignancy with a high mortality rate. PDAC is the third-/fourth-leading cause of cancer-related deaths in the United States, Europe, and Japan.[1–3] Although several efforts have been made to establish effective therapies for PDAC, the 5-year survival rate in PDAC is ∼5% to 10%.[2,4,5] To overcome the limitations in PDAC treatment, it is important to understand the molecular mechanism underlying PDAC formation and identify suitable therapeutic targets. Reportedly, human PDAC involves gene mutations in 10 core signaling pathways, with the Notch signaling pathway considered as one of the main pathways.[6] Hairy and enhancer of split-1 (HES1) is the primary downstream target of the Notch signaling pathway and is known to play important roles in cell and tissue development.[7] However, the role of HES1 in PDAC remains controversial.

In the development of the pancreas, HES1 is expressed in stem/progenitor cells at the embryonic stage and is considered to be important in the maintenance of these cells as well as in deciding their fate.[8,9] Indeed, global *Hes1* knockout (KO) mice show pancreatic hypoplasia, which indicates the essential role of *Hes1* in pancreas development.[9] Although HES1 expression is limited to duct/centroacinar cells in the adult pancreas under normal conditions, it is also observed in acinar-to-ductal metaplasia (ADM),[10,11] which represents a state of temporal dedifferentiation of acinar cells under inflammatory conditions. We previously

***Abbreviations used in this paper:*** **Ad-Cre-GFP, Cre recombinase and green fluorescent protein-expressing adenovirus; Ad-GFP, green fluorescent protein-expressing adenovirus; ADM, acinar-to-ductal metaplasia; Aldh, aldehyde dehydrogenase; ChIP-qPCR, chromatin immunoprecipitation-quantitative polymerase chain reaction; CK, cytokeratin; DMEM, Dulbecco's modified Eagle medium; ERT2, mutated estrogen receptor; FACS, fluorescence-activated cell sorting; FBS, fetal bovine serum; GFP, green fluorescent protein; HES1, hairy and enhancer of split-1; *Hes1*KO, Hes1-negative cells; Hnf1$\beta$;Hes1KO, *Hnf1$\beta$-CreER-T2;Hes1$^{flox/flox}$*; IHC, immunohistochemistry; KO, knockout; mRNA, messenger RNA; MUC5AC, mucin 5, subtype AC; PanIN, pancreatic intraepithelial neoplasia; PDAC, pancreatic ductal adenocarcinoma; Pdx1;Hes1KO, *Pdx1-Flp;FSF-R26$^{CAG\text{-}CreERT2}$;Hes1$^{flox/flox}$*; Pdx1;Hes1WT, *Pdx1-Flp;Hes1$^{flox/flox}$*; Pdx1K;Hes1KO, *Pdx1-Flp;FSF-R26$^{CAG\text{-}CreERT2}$;FSF-Kras$^{G12D}$;Hes1$^{flox/flox}$*; Pdx1K;Hes1WT, *Pdx1-Flp;FSF-Kras$^{G12D}$;Hes1$^{flox/flox}$*; Pdx1KP;Hes1KO, *Pdx1-Flp;FSF-R26$^{CAG\text{-}CreERT2}$;FSF-Kras$^{G12D}$;Trp53$^{frt/+}$;Hes1$^{flox/flox}$*; Pdx1KP;Hes1WT, *Pdx1-Flp;FSF-Kras$^{G12D}$;Trp53$^{frt/+}$;Hes1$^{flox/flox}$*; qRT-PCR, quantitative reverse-transcription polymerase chain reaction; RNA-seq, RNA sequencing; WT, wild-type.**

**Most current article**



0016-5085
https://doi.org/10.1053/j.gastro.2022.08.048

**WHAT YOU NEED TO KNOW**

BACKGROUND AND CONTEXT

The roles of Hes1 in adult pancreas and pancreatic ductal adenocarcinoma remain controversial.

NEW FINDINGS

Under inflammatory condition, loss of Hes1 in centroacinar/terminal duct resulted in pancreatic atrophy. Hes1 deletion inhibited pancreatic intraepithelial neoplasia/pancreatic ductal adenocarcinoma initiation, while it could promote pancreatic intraepithelial neoplasia/pancreatic ductal adenocarcinoma progression.

LIMITATIONS

This study was performed using mice, murine cells, and human RNA sequencing data, hence further studies are warranted in humans.

IMPACT

Hes1 plays distinct roles in pancreas based on the cellular context and tumor phase. Hes1 plays an important role in pancreatic regeneration after inflammation, whereas Hes1 has a suppressive role in pancreatic ductal adenocarcinoma progression.



reported that HES1 is nonessential for the maintenance of adult acinar cells under normal and inflammatory conditions.[11] In contrast, another study showed that *Hes1* deletion in the adult duct cells of *Sox9-IRES-CreERT2* knock-in mice promoted transdifferentiation from duct to acinar cells with *Sox9* suppression.[12] Therefore, the precise roles of HES1 in the adult pancreas are yet to be determined.

PDAC is believed to primarily form from acinar cells bearing mutant *Kras* that transform into pancreatic intraepithelial neoplasia (PanIN) through ADM.[13] In pancreatic tumor development, HES1 expression commences at the ADM stage and continues during PanIN and PDAC formation,[10,14] suggesting the involvement of *Hes1* in both PDAC initiation and progression. However, 2 conflicting reports have been published on the role of HES1 in pancreatic tumorigenesis.[11,15] One report showed that simultaneous *Hes1* deletion and $Kras^{G12D}$ induction in the whole embryonal pancreas accelerated $Kras^{G12D}$-induced PDAC formation.[15] In contrast, simultaneous *Hes1* ablation with $Kras^{G12D}$ induction in adult acinar cells was shown to induce tumor suppression, and HES1 in acinar cell-derived ADM was shown to be essential for PanIN formation in mice.[11] Both reports were based on studies on the $Kras^{G12D}$-driven PDAC mouse model, but the timing and the cells used for $Kras^{G12D}$ induction and *Hes1* ablation were different.

Given that HES1 is involved in pancreatic development, our strategy with conditional gene modification in adults may be more suitable for analyzing pancreatic tumorigenesis. Furthermore, to clarify the roles of HES1 in PDAC initiation and progression more precisely, it is necessary to induce *Hes1* deletion independently of $Kras^{G12D}$ induction. However, in Cre-loxP PanIN/PDAC mouse models, it was impossible to induce *Hes1* deletion independently of $Kras^{G12D}$ induction.

In the present study, we combined a flippase-recombinase-recombination target and a CreERT2-loxP recombination system[16] to generate a dual-recombinase mouse model for conditional *Hes1* deletion in the adult pancreas at various stages of tumor development independent of mutant *Kras* induction. Using this dual-recombinase mouse model, we confirmed that HES1 is not required for the maintenance of the adult pancreas under normal settings, but is indispensable for regeneration after caerulein-induced acute pancreatitis. With respect to tumor development, we found that the loss of *Hes1* expression suppresses PanIN formation; however, once PanINs develop, the loss of *Hes1* expression promotes tumor progression. Collectively, our data indicate the context-dependent roles of *Hes1* in the adult pancreas as well as in pancreatic tumor formation.

## Methods

### Mice

The generation of *Hes1* flox mice (generously provided by Ryoichiro Kageyama, Institute for Virus Research, Kyoto University, Kyoto, Japan),[17] *LSL-*$Kras^{G12D}$ mice (The Jackson Laboratory, Bar Harbor, ME),[18] *FSF-*$Kras^{G12D}$ mice,[16] *Pdx1-Flp* mice,[16] *FSF-*$R26^{CAG-CreERT2}$ mice,[16] $Trp53^{frt/+}$ mice,[19] and *Hnf1β-CreERT2* mice (generously provided by Jorge Ferrer, Imperial College, London, United Kingdom)[20] has been reported previously. The mice were maintained in a specific pathogen-free facility at the Kyoto University Faculty of Medicine (Kyoto, Japan). Male and female mice were both used without any specific criteria, and randomization and blinding were not used in the analysis of the mouse model.

Acute pancreatitis was induced by 8-hourly intraperitoneal injections of 100 μg/kg caerulein (Sigma-Aldrich, St Louis, MO) dissolved in phosphate-buffered saline for 2 consecutive days. For caerulein-induced pancreatitis, the mice were provided ad libitum access to food and water. Tamoxifen (Sigma-Aldrich) was administered at a dose of 4 to 6 mg for each mouse by subcutaneous injection to mice carrying the *FSF-*$R26^{CAG-CreERT2}$ gene and its control, or 10 mg of tamoxifen was administered via oral gavage for 5 days to mice carrying the *Hnf1β-CreERT2* gene and its control.

Serum amylase levels were measured using SPOTCHEM EZ (Arkray, Kyoto, Japan) according to the manufacturer's instructions.

### Histology

Mice were euthanized, and pancreatic tissues were harvested. Pancreatic tissues were fixed in 10% neutral phosphate-buffered formalin and embedded in paraffin. The paraffin-embedded tissues were cut into 5-μm sections. For histologic and immunohistochemistry (IHC) analyses, the paraffin-embedded sections were stained with H&E, Alcian blue, nuclear fast red (Kirkegaard & Perry Laboratories, Gaithersburg, MD), Masson's trichrome solution (Muto Pure Chemical, Tokyo, Japan), and IHC.

IHC analysis was performed using standard methods. The sections were treated overnight with primary antibodies at 4°C. For detection, an EnVision+ kit (Dako, Glostrup, Denmark) or VECTASTAIN Elite ABC kit (Vector Laboratories, Burlingame,

CA) was used, according to the manufacturer's instructions. For all immunolabeling experiments, the sections were developed using the Liquid DAB+ Substrate Chromogen System (Dako) and counterstained with hematoxylin. The primary antibodies for IHC are listed in Supplementary Table 1. The HES1 primary antibody was provided by Tetsuo Sudo[21] (Toray Industries, Tokyo, Japan).

### Morphometric Quantification

Morphometric analysis was performed using the ImageJ 1.53a software (National Institutes of Health, Bethesda, MD). For specific lesion quantification, PanIN, PDAC, and pancreatic tissues in each field were encircled manually, and the respective areas were calculated using the imaging software. For determining the number of cells expressing cleaved caspase-3 and Ki-67, labeled cells from 6 to 10 optical fields of each pancreas were counted manually.

### Cell Culture

To isolate primary PDAC cells, fresh tumors were minced using sterile razor blades and maintained in Dulbecco's modified Eagle medium (DMEM; Thermo Fisher Scientific, Waltham, MA) supplemented with 10% fetal bovine serum (FBS; Thermo Fisher Scientific) and a 1% penicillin/streptomycin antibiotic mixture (Thermo Fisher Scientific) at 37°C under a humidified atmosphere with 5% $CO_2$.

### Murine Model of Hepatic Metastases

A hepatic metastasis model was established by intrasplenic injection of $3 \times 10^5$ PDAC cells in 100 $\mu$L DMEM. A small left abdominal flank incision was made where the spleen was exteriorized for the intrasplenic injection under general anesthesia. The prepared cells were injected into the spleen of 8-week-old female C57BL/6N mice (Japan SLC, Shizuoka, Japan) with a 27-gauge needle. *Hes1*-wild-type (WT) and *Hes1*-KO PDAC cells were injected in 3 mice each. The livers were assessed 3 weeks after injection.

### Isolation of Aldehyde Dehydrogenase-Positive Cells Using Fluorescence-Activated Cell Sorting

Aldehyde dehydrogenase (Aldh)-positive cells were isolated using fluorescence-activated cell sorting (FACS), according to a previously described method.[22] Adult mouse pancreata were dissected, washed in iced Hank's balanced salt solution (Thermo Fisher Scientific), and minced into small pieces. The pancreata tissues were digested with 1 mg/mL collagenase D (Roche, Basel, Switzerland) dissolved in DMEM and supplemented with 2 U/mL deoxyribonuclease I (Promega, Madison, WI) and 1% bovine serum albumin (FUJIFILM Wako Pure Chemical Corp, Osaka, Japan) for 20 minutes on a shaker at 37°C. The cells were pipetted through a 1-mL pipette tip every 5 minutes. The reaction was terminated by adding ice-cold DMEM supplemented with 5% FBS. The cells were then passed through a 100-$\mu$m, 70-$\mu$m, and 40-$\mu$m cell strainer sequentially, centrifuged at 300*g* for 3 minutes at 4°C, resuspended in DMEM, and counted.

The cell suspension was treated with the ALDEFLUOR reagent (STEMCELL Technologies, Vancouver, British Columbia, Canada) for 30 minutes in the dark at 37°C on a shaker. Diethylaminobenzaldehyde, an inhibitor of Aldh, was also added to the cells in the negative control group. After the ALDEFLUOR reaction, the cells were centrifuged and resuspended in DMEM. FACS Aria II (Becton Dickinson, Franklin Lakes, NJ) was used for FACS. The cell debris were removed by forward scatter and side scatter. Aldh-positive cells were isolated based on ALDEFLUOR activity (fluorescein isothiocyanate channel) and collected in 100% FBS supplemented with 1% penicillin/streptomycin.

### Statistics

Statistical analysis was performed using the JMP (SAS Institute, Inc, Cary, NC), GraphPad Prism (GraphPad Software, San Diego, CA), or Excel (Microsoft, Redmond, WA) software programs. A 2-tailed Student's *t* test was used to analyze differences between 2 groups for continuous data. The $\chi^2$ test was used for the analysis of categorical data. Statistical significance was set at $P < .05$. Data are presented in as mean ± standard error of the mean.

### Study Approval

All animal experiments were approved by the Ethics Committee for Animal Experiments and performed under the Guidelines for Animal Experiments of Kyoto University (Med-Kyo 16207, 17196, 18546, 19234, 20267, and 21213).

## Results

### Hairy and Enhancer of Split-1 Is Not Essential for Homeostasis of Adult Pancreas Under Normal Conditions

By inducing *Hes1* deletion in acinar cells, we previously reported that HES1 is not essential for homeostasis of adult acinar cells.[11] However, the effect of *Hes1* deletion in the whole adult pancreas has not been evaluated.[9,15,23] To elucidate the roles of HES1 in the adult mouse pancreas, we adopted a dual-recombinase system[16] to generate *Pdx1-Flp;FSF-R26$^{CAG\text{-}CreERT2}$;Hes1$^{flox/flox}$* mice (referred to as Pdx1;Hes1KO), with *Hes1* gene deletion in all adult pancreatic cells, including acinar cells, centroacinar/terminal duct cells, duct cells, and islet cells, in a tamoxifen-dependent manner (Figure 1*A*). We also generated *Pdx1-Flp;Hes1$^{flox/flox}$* mice as controls (referred to as Pdx1;Hes1WT).

One-month-old Pdx1;Hes1KO and Pdx1;Hes1WT mice were subcutaneously administered 4 mg of tamoxifen for 5 consecutive days and evaluated 1 and 6 months later (Figure 1*B*). To confirm *Hes1* deletion, HES1 expression was examined using IHC. As previously reported,[10] HES1 was expressed in the duct/centroacinar cells of Pdx1;Hes1WT mice (Figure 1*C*). Conversely, HES1 was not expressed in most of the duct/centroacinar cells of Pdx1;Hes1KO mice, which confirmed successful recombination. Compared with Pdx1;Hes1WT mice, Pdx1;Hes1KO mice showed no obvious morphologic differences in the pancreatic acinar cells, duct cells, and islet cells, as evaluated using H&E staining and cytokeratin (CK) 19, amylase, glucagon, and insulin IHC at 1 and 6 months (Figure 1*C*). Moreover, there was no

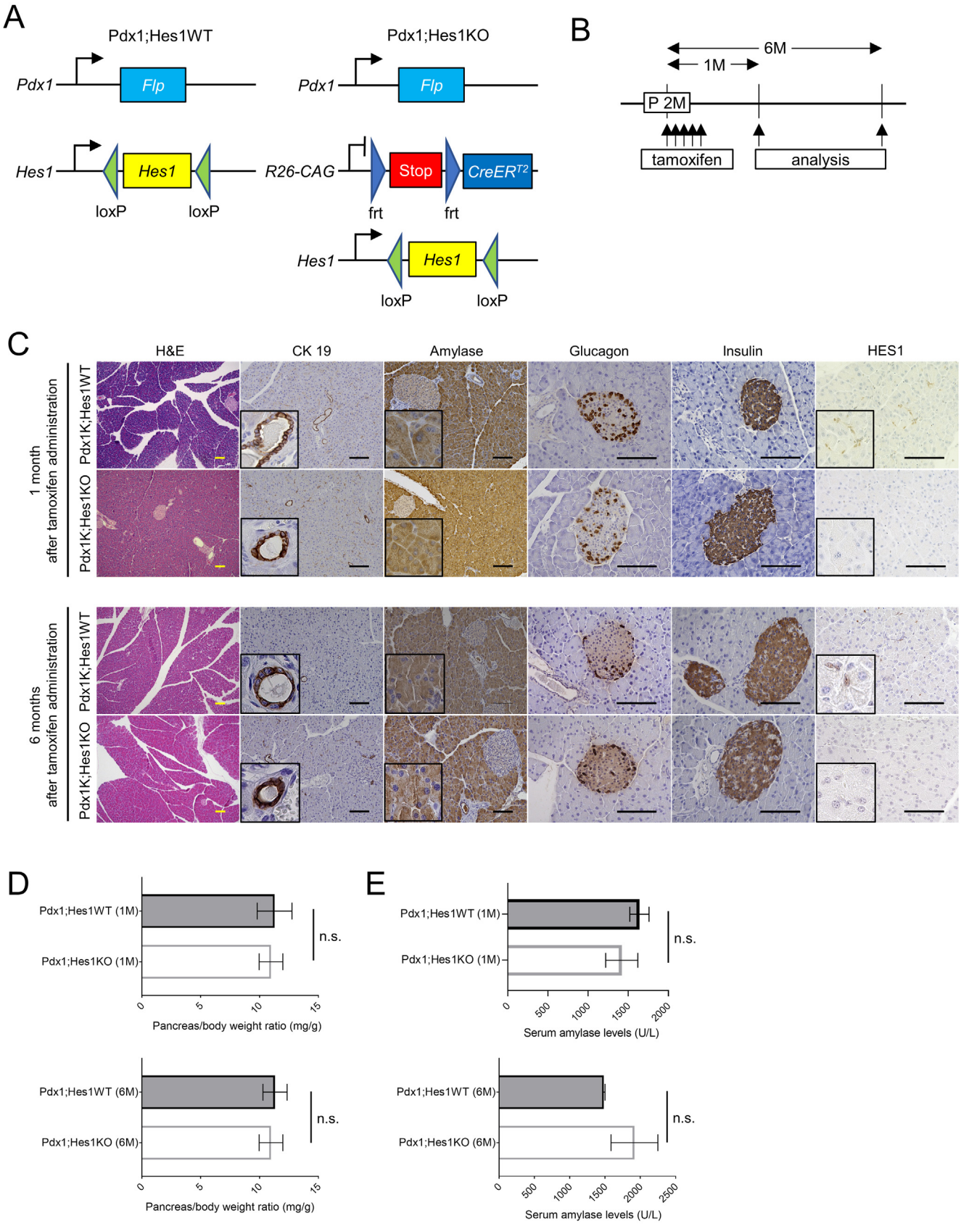
A
Pdx1;Hes1WT
Pdx1
Flp
Hes1
Hes1
loxP
loxP
Pdx1;Hes1KO
Pdx1
Flp
R26-CAG
Stop
CreER^T2
frt
frt
Hes1
Hes1
loxP
loxP
B
6M
1M
P 2M
tamoxifen
analysis
C
H&E
CK 19
Amylase
Glucagon
Insulin
HES1
1 month after tamoxifen administration
Pdx1K;Hes1WT
Pdx1K;Hes1KO
6 months after tamoxifen administration
Pdx1K;Hes1WT
Pdx1K;Hes1KO
D
Pdx1;Hes1WT (1M)
Pdx1;Hes1KO (1M)
n.s.
0
5
10
15
Pancreas/body weight ratio (mg/g)
Pdx1;Hes1WT (6M)
Pdx1;Hes1KO (6M)
n.s.
0
5
10
15
Pancreas/body weight ratio (mg/g)
E
Pdx1;Hes1WT (1M)
Pdx1;Hes1KO (1M)
n.s.
0
500
1000
1500
2000
Serum amylase levels (U/L)
Pdx1;Hes1WT (6M)
Pdx1;Hes1KO (6M)
n.s.
0
500
1000
1500
2000
2500
Serum amylase levels (U/L)

significant difference in the pancreas/body weight ratio (Figure 1*D*) and serum amylase levels (Figure 1*E*) between Pdx1;Hes1KO and Pdx1;Hes1WT mice.

We previously reported that *Hes1* deletion from the embryonic period causes a reduction of centroacinar cells, which leads to pancreatic atrophy.[23] In this study, we examined whether *Hes1* deletion in the adult pancreas affects the number of centroacinar/terminal duct cells. We evaluated centroacinar cells by sex determining region Y-box transcription factor 9 (SOX9) expressions in peripheral acinar cells. IHC of SOX9 in peripheral acinar cells showed no significant difference between Pdx1;Hes1KO and Pdx1;Hes1WT mice (Supplementary Figure 1*A*). Accordingly, we concluded that HES1 is not essential for homeostasis in the adult pancreas under normal conditions.

## Hairy and Enhancer of Split-1 Is Essential for Regeneration of Pancreatic Tissue After Acute Pancreatitis

Next, we evaluated the role of HES1 in pancreatic regeneration after acute pancreatitis. We previously reported that *Hes1* deletion in adult acinar cells does not affect regeneration after caerulein-induced acute pancreatitis.[11] However, another study showed that *Hes1* deletion in the whole pancreas during the embryonic stage impaired regeneration after caerulein-induced acute pancreatitis.[15] The main differences between the findings from the 2 studies were attributed to *Hes1* deletion during the adult or embryonic period and in acinar cells or the whole pancreas.

We used Pdx1;Hes1KO and Pdx1;Hes1WT mice, as described above. To examine the effect of *Hes1* deletion in the adult whole pancreas on regeneration after acute pancreatitis, *Hes1* deletion was induced in adult whole pancreatic cells by tamoxifen administration at age 8 weeks, followed by the induction of pancreatitis by treatment with caerulein (Figure 2*A*). Compared with Pdx1;Hes1WT mice, Pdx1;Hes1KO mice showed significant atrophy in the pancreas at 7 days after caerulein administration (Figure 2*B*), and the pancreas/body weight ratio was significantly smaller in Pdx1;Hes1KO mice than in Pdx1;Hes1WT mice (Figure 2*C*). Inflammatory cells infiltrated more frequently in Pdx1;Hes1KO mice than in Pdx1;Hes1WT mice at 2 days after caerulein-induced pancreatitis (Supplementary Figure 2*A*). To explore the mechanism underlying atrophy, we examined the pancreas at 2 and 7 days after caerulein administration. The pancreas of Pdx1;Hes1KO and Pdx1;Hes1WT mice showed widespread ADM lesions, expressing both CK19 and amylase (Figure 2*D*). The CK19-positive area was significantly larger in Pdx1;Hes1KO mice than in Pdx1;Hes1WT mice at 7 days after caerulein-induced pancreatitis (Supplementary Figure 2*B*), showing persistence of regeneration in Pdx1;Hes1KO mice. Moreover, the number of cleaved caspase-3–positive cells was significantly higher in Pdx1;Hes1KO mice at 2 days after caerulein administration (Figure 2*D* and *E*), indicating that apoptosis occurred more frequently in Pdx1;Hes1KO mice than in Pdx1;Hes1WT mice. Proliferation analysis using the Ki-67 marker did not show any significant difference (data not shown).

We previously showed that *Hes1* deletion in adult acinar cells does not affect pancreatic regeneration after caerulein-induced pancreatitis.[11] Accordingly, we next explored whether *Hes1* deletion in adult duct cells exerts any effect. We induced *Hes1* deletion in adult pancreatic duct cells by tamoxifen administration in *Hnf1β-CreERT2;Hes1*$^{flox/flox}$ mice (referred to as Hnf1$\beta$;Hes1KO) and then induced pancreatitis by treating with caerulein (Supplementary Figure 3*A* and *B*). No difference was observed between Hnf1$\beta$;Hes1KO and Hnf1$\beta$;Hes1WT mice with respect to morphology and the pancreas/body weight ratio (Supplementary Figure 3*C* and *D*). Accordingly, we hypothesized that HES1 does not play an important role in acinar cells or duct cells during pancreas regeneration; therefore, we focused on centroacinar/terminal duct cells, which exhibit a strong proliferative response to caerulein-induced pancreatitis.[24]

## Hairy and Enhancer of Split-1 Is Essential for the Proliferation of Centroacinar/Terminal Duct Cells

Centroacinar/terminal duct cells express Aldh and can be cultured as organoids.[22] We collected centroacinar/terminal duct cells from *Hes1*$^{flox/flox}$ mice by FACS using the ALDEFLUOR reagent and cultured organoids (Figure 3*A*). Adenoviral vectors were used to test the effect of *Hes1* deletion in organoids. The organoids were dissociated into single cells, infected with Cre recombinase and green fluorescent protein (GFP)-expressing adenovirus vectors (Ad-Cre-GFP) or only GFP-expressing adenovirus (Ad-GFP), and cultured for 10 days. First, we examined the efficacy of *Hes1* deletion on day 0 using quantitative reverse-transcription polymerase chain reaction (qRT-PCR) and observed considerable reduction in *Hes1* messenger (m)RNA expression (Figure 3*B*). Ten days after adenoviral infection, the *Hes1*-positive cells (Hes1WT) formed multiple organoids, whereas the *Hes1*-negative cells (Hes1KO) formed few organoids (Figure 3*C*). The numbers of organoids of Hes1KO were significantly lower than that of Hes1WT. The size of Hes1KO organoids also tended to be smaller than that of Hes1WT organoids; however, it was not significant

**Figure 1.** HES1 is not essential for homeostasis in the adult pancreas under normal conditions. (*A*) Genetic strategy for inducing *Hes1* deletion in the adult pancreas via time-specific tamoxifen-mediated CreERT2 activation in Pdx1;Hes1WT and Pdx1;Hes1KO mice. (*B*) Schematic representation of the experimental design for tamoxifen administration and analysis. M, month. (*C*) H&E and IHC staining for CK19, amylase, glucagon, insulin, and HES1 at 1 month and 6 months after tamoxifen administration. Magnified images are shown in the *inset*. *Scale bars*, 100 $\mu$m. (*D*) Ratio of pancreas weight to body weight in Pdx1;Hes1WT and Pdx1;Hes1KO mice at 1 month and 6 months after tamoxifen administration (n = 3 in each group). (*E*) Serum amylase levels in Pdx1;Hes1WT and Pdx1;Hes1KO mice at 1 month and 6 months after tamoxifen administration (n = 5 in each group). Plotted values represent the mean ± standard deviation. n.s., not significant.

(Figure 3*C*). The cell proliferation assay revealed significantly lower proliferation in Hes1KO organoids than in Hes1WT organoids (Figure 3*D*). Moreover, we evaluated *Hes1* mRNA expression in the organoids at 10 days after adenoviral infection and confirmed *Hes1* mRNA up-regulation in both Hes1WT and Hes1KO organoids

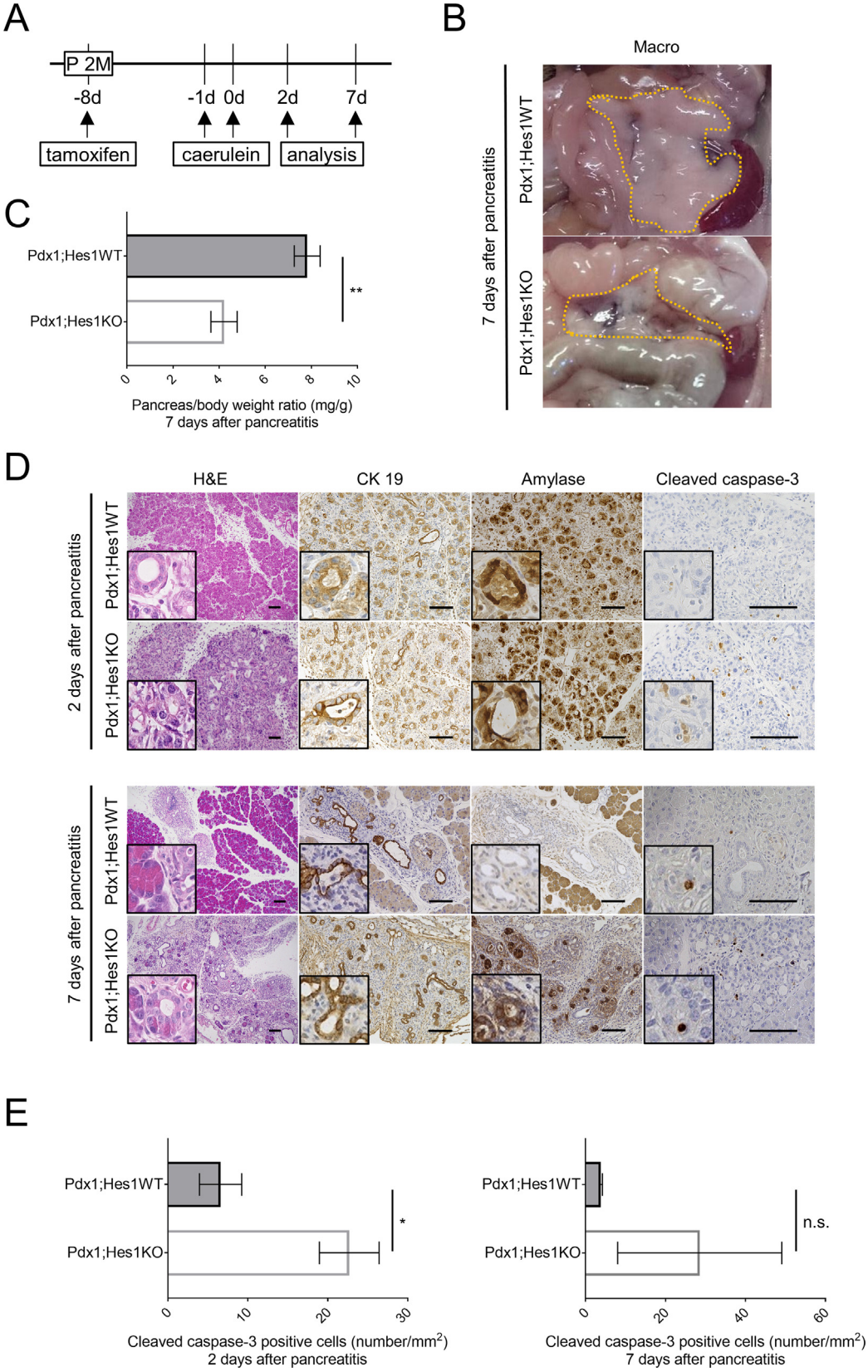

(Figure 3*B*), suggesting that the cells escaping *Hes1* deletion mainly formed Hes1KO organoids at day10. These results indicated that *Hes1* is essential for the proliferation of centroacinar/terminal duct cells and that *Hes1* deletion in centroacinar/terminal duct cells may impair regeneration after acute pancreatitis.

## Hairy and Enhancer of Split-1 Promotes Pancreatic Intraepithelial Neoplasia Initiation but Inhibits Its Progression

Next, we explored the role of HES1 in pancreatic tumor formation using the $Kras^{G12D}$-driven mouse PanIN model. We previously reported that *Hes1* deletion with concomitant $Kras^{G12D}$ activation in adult acinar cells suppresses $Kras^{G12D}$-induced PanIN formation through the depletion of *Hes1* in ADM,[11] indicating that *Hes1* plays an essential role in PanIN initiation in ADM derived from acinar cells. In this study, we generated *Pdx1-Flp;FSF-R26*$^{CAG\text{-}CreERT2}$*;FSF-Kras*$^{G12D}$*;Hes1*$^{flox/flox}$ (referred to as Pdx1K;Hes1KO) mice and *Pdx1-Flp;FSF-Kras*$^{G12D}$*;Hes1*$^{flox/flox}$ (referred to as Pdx1K;Hes1WT) mice (Figure 4*A*).

First, we found that PanIN formation was rarely observed at the age of 6 weeks, but was frequently observed at 3 months in all mice mentioned above, which indicated that PanIN formation commences between 6 weeks and 3 months (Supplementary Figure 4*A*–*C*). To confirm the stimulatory role of HES1 in PanIN initiation in this model, tamoxifen was administered to 1-month-old mice to induce *Hes1* deletion before PanIN formation (Figure 4*B*). As expected, at 3 months, PanIN was rarely detected in Pdx1K;Hes1KO compared with Pdx1K;Hes1WT (Figure 4*C* and *D*). Next, tamoxifen was administered to 3-month-old PanIN-bearing mice to induce *Hes1* deletion (Figure 4*E*). Surprisingly, 3 months after tamoxifen administration, Alcian blue staining revealed the presence of more PanINs in Pdx1K;Hes1KO mice than in Pdx1K;Hes1WT mice (Figure 4*F* and *G*), which contrasted with the results obtained with *Hes1* deletion before PanIN development. Collectively, the findings indicated that HES1 enhances PanIN initiation but inhibits its progression, suggesting the dual roles of HES1 in PanIN formation, depending on the stage of tumor development.

## Hairy and Enhancer of Split-1 Promotes Pancreatic Intraepithelial Neoplasia Initiation and Inhibits Its Progression in Caerulein-Induced Pancreatitis

To elucidate whether HES1 is involved in pancreatitis-induced PanIN formation, we investigated PanIN formation after caerulein treatment. Previous studies have demonstrated that pancreatic inflammation, including that observed in chronic pancreatitis, an etiological factor for PDAC, accelerates the development of PanINs in the presence of mutant Kras.[25,26] In the PanIN mouse model used in this study (Pdx1K;Hes1KO and Pdx1K;Hes1WT mice) (Figure 4*A*), PanIN formation commenced between 6 weeks and 3 months (Supplementary Figure 4*A*–*C*).

In one group (referred to as initiation group), Pdx1K;Hes1KO and Pdx1K;Hes1WT mice were administered tamoxifen at the age of 6 weeks (limited PanIN formation was observed at this point, as described above), and caerulein was administered for 2 consecutive days at 1 week after tamoxifen administration (Figure 5*A*). In this group, *Hes1* deletion was induced before PanIN formation; accordingly, we evaluated the role of HES1 in PanIN initiation. In the other group (referred to as progression group), Pdx1K;Hes1KO and Pdx1K;Hes1WT mice were administered caerulein at the age of 6 weeks to induce PanIN development and were then treated with tamoxifen at 1 week after caerulein administration (Figure 5*A*). In this group, *Hes1* deletion was induced after PanIN formation. Therefore, we could evaluate the role of HES1 in PanIN progression.

Pancreatic tissues were assessed at age 5 months in both groups. In the initiation group, Pdx1K;Hes1KO mice showed a significantly smaller area of PanINs than Pdx1K;Hes1WT mice (Figure 5*B* and *C*). In contrast, in the progression group, Pdx1K;Hes1KO mice showed a significantly larger area of PanINs than Pdx1K;Hes1WT mice (Figure 5*B* and *C*). These results indicate that HES1 accelerates PanIN initiation but inhibits its progression after caerulein-induced pancreatitis. These results were consistent with the results of the caerulein-unrelated PanIN model described in the previous subsection; therefore, the roles of HES1 differ depending on the stage of tumor initiation and progression.

## Hairy and Enhancer of Split-1 Suppresses Pancreatic Ductal Adenocarcinoma Progression

To investigate the role of HES1 in PDAC progression, we generated a PDAC mouse model with a mutated $Kras^{G12D}$ oncogene and deletion of 1 allele of the *Trp53* gene (*Pdx1-Flp;FSF-R26*$^{CAG\text{-}CreERT2}$*;FSF-Kras*$^{G12D}$*;Trp53*$^{frt/+}$*;Hes1*$^{flox/flox}$ [referred to as Pdx1KP;Hes1KO] mice and *Pdx1-Flp;FSF-Kras*$^{G12D}$*;Trp53*$^{frt/+}$*;Hes1*$^{flox/flox}$ [referred to as Pdx1KP;Hes1WT] mice) (Figure 6*A*). These mice showed the formation of several PanINs and eventually developed PDAC at ~3 months after birth (data not shown). The mice were administered tamoxifen at the age of 3 months and analyzed

**Figure 2.** HES1 is essential for tissue regeneration after acute pancreatitis. (*A*) Schematic representation of the experimental design for tamoxifen administration, induction of caerulein-induced acute pancreatitis, and analysis. M, month; d, day. (*B*) Macroscopic view of the pancreas at 7 days after caerulein-induced acute pancreatitis. *Orange dash lines* indicate pancreas area. (*C*) Ratio of pancreas weight to body weight in Pdx1;Hes1WT (n = 6) and Pdx1;Hes1KO (n = 5) mice at 7 days after caerulein-induced acute pancreatitis. (*D*) H&E staining; IHC staining for CK19, amylase, and cleaved caspase-3 in pancreatic tissues at 2 and 7 days after caerulein-induced acute pancreatitis. *Scale bars*, 100 $\mu$m. (*E*) Quantification of cleaved caspase-3–positive cells in the pancreas at 2 and 7 days after caerulein-induced acute pancreatitis (n = 3 in each group). Plotted values represent the mean ± standard deviation. n.s., not significant; $^{*}P < .05$; $^{**}P < .01$.

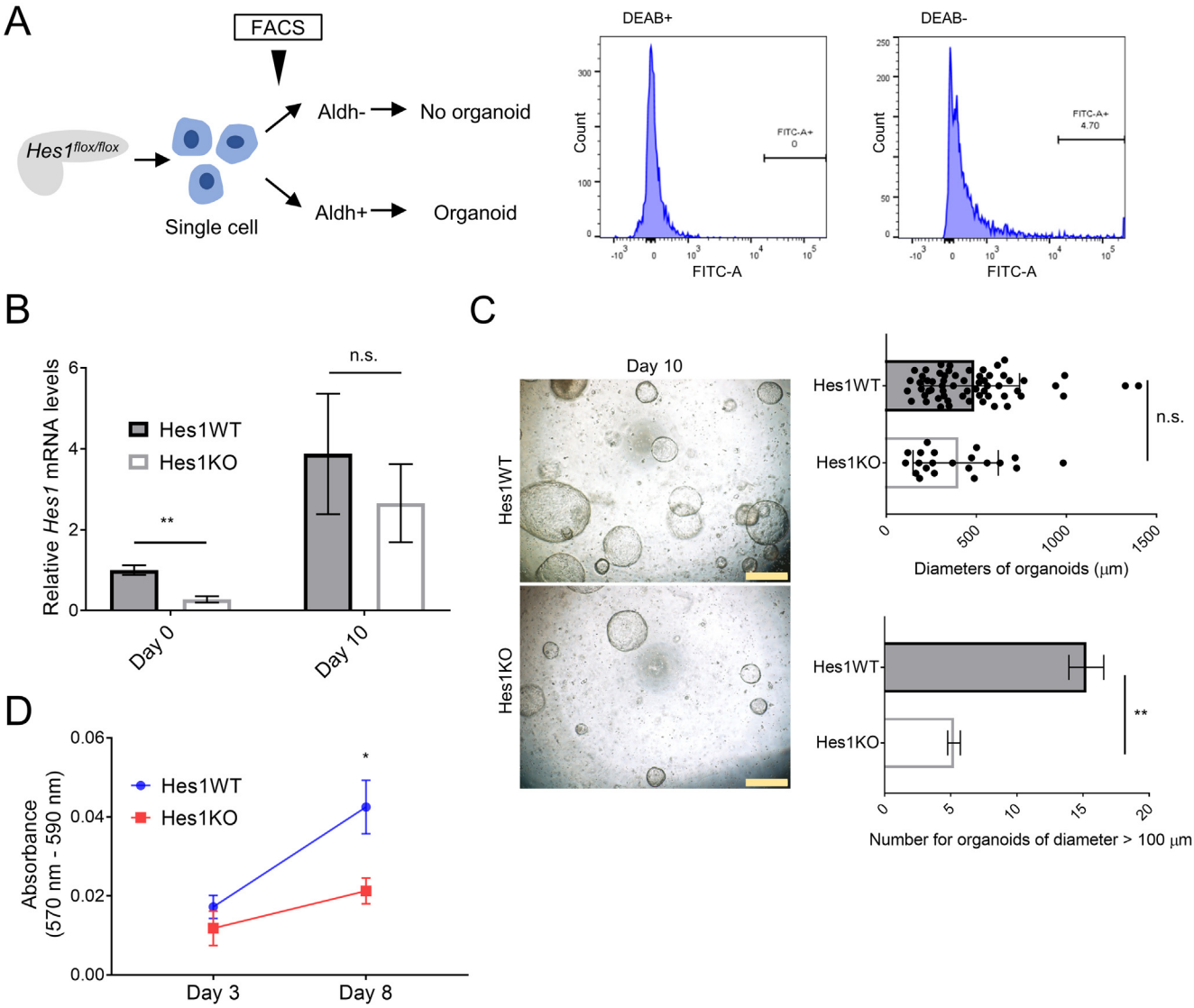


**Figure 3.** HES1 is essential for the proliferation of centroacinar/terminal duct cells. (*A*) Schematic representation of the experimental design for organoid culture (*left*), and histogram showing the results of the flow cytometry experiment for the isolation of cells with high Aldh activity among pancreatic cells of *Hes1*$^{flox/flox}$ mice with (+) or without (−) diethylaminobenzaldehyde (DEAB) treatment (*right*). FITC, fluorescein isothiocyanate. (*B*) Evaluation of *Hes1* mRNA expression in organoids from *Hes1*-expressing cells (Hes1WT) and *Hes1*-deleted cells (Hes1KO) using qRT-PCR (n = 3 in each group). (*C*) Organoids developed from Hes1WT and Hes1KO cells and cultured for 10 days (*left*). *Scale bars*, 500 μm. Evaluation of size (*right top*) and number (*right bottom*) of organoids with a diameter of >100 μm from Hes1WT and Hes1KO. Organoids were counted per field of vision. Plotted values represent the mean ± standard deviation. (*D*) Cell proliferation assay of Hes1WT and Hes1KO organoids (n = 3 in each group). *$P < .05$; **$P < .01$; n.s., not significant.

3 months later (Figure 6*B*). *Hes1* deletion was confirmed by IHC (Figure 6*C* and Supplementary Figure 5*A*). Both the area and the number of PDACs in Pdx1KP;Hes1KO mice were significantly higher than those in Pdx1KP;Hes1WT mice, and Pdx1KP;Hes1KO mice tended to show a lower survival rate (Figure 6*C*–*F*). These data suggest that *Hes1* deletion promotes PanIN/PDAC progression.

Hes1 is the primary target of the Notch signaling pathway; therefore, to ascertain whether Notch signaling is involved in this tumor setting, we evaluated the expression of Notch signaling components by IHC and found no differences in Notch1-4 and Jag 1 expression between Pdx1KP;Hes1KO and Pdx1KP;Hes1WT PDAC mice (Supplementary Figure 5*B*). The data suggest that Hes1 is regulated independently of Notch signaling in PDAC. To confirm this hypothesis, we evaluated the correlation between Hes1 and Notch ligands and receptors mRNA expressions in human pancreatic cancer using The Cancer Genome Atlas pancreatic cancer database. As we expected, no correlation was found between mRNA expression of Hes1 and Notch components (Supplementary Figure 6).

To further analyze the role of HES1 in PDAC progression, we established 3 PDAC cell lines from the tumors of 3 *Pdx1-Flp;FSF-Kras*$^{G12D}$*;Trp53*$^{frt/+}$*;Hes1*$^{flox/flox}$ mice. Each cell line was Ad-Cre-GFP or only Ad-GFP as a control; the cells were named Hes1KO #1–3 and Hes1WT #1–3 PDAC cells,

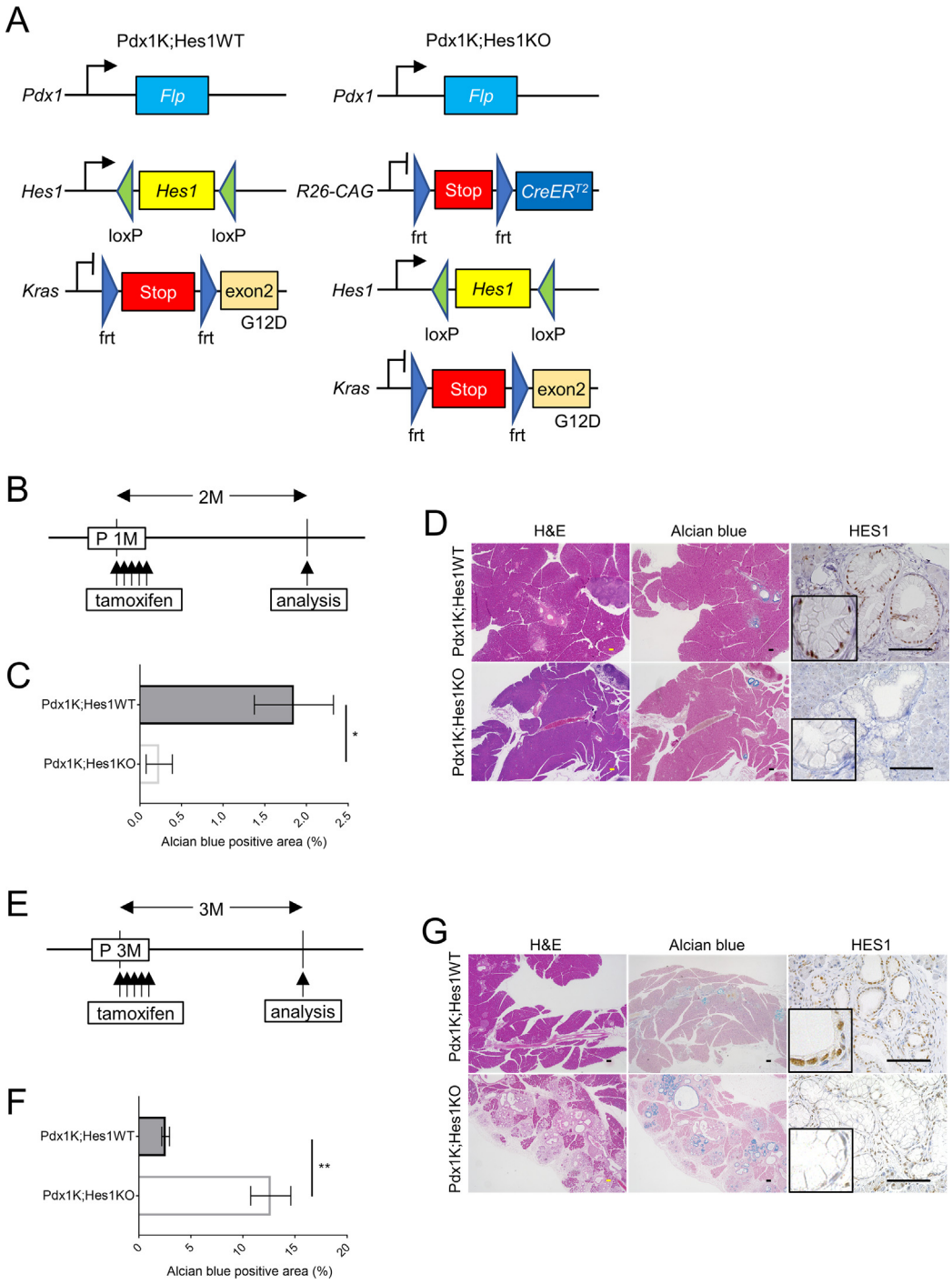


**Figure 4.** HES1 promotes PanIN initiation but inhibits its progression. (*A*) Genetic strategy for *Hes1* deletion in the adult pancreas via time-specific tamoxifen-mediated CreERT2 activation after embryonal pancreatic $Kras^{G12D}$ induction in Pdx1K;Hes1WT and Pdx1K;Hes1KO mice. (*B* and *E*) Schematic representation of the experimental design for tamoxifen administration and analysis. M, month. (*C*) Percentage of Alcian blue-positive area in the pancreas (n = 3 in each group). (*D* and *G*) H&E, Alcian blue, and IHC staining for HES1 in the pancreatic tissues. All PanINs observed in those mice were classified as low-grade PanIN. *Scale bars*, 100 $\mu$m. (*F*) Percentage of Alcian blue-positive area in the pancreas (n = 5, in each group). Plotted values represent the mean ± standard deviation. $^{*}P < .05$; $^{**}P < .01$.

respectively. Sufficient *Hes1* deletion was detected using qRT-PCR (Figure 6*G*). The proliferation of Hes1WT and Hes1KO PDAC cells was measured using the 3-(4,5-dimethylthiazol-2-yl)-5-(3-carboxymethoxyphenyl)-2-(4-sulfophenyl)-2H-tetrazolium (MTS) assay, and no significant differences were observed between Hes1WT and Hes1KO PDAC cells (Figure 6*H*).

We further assessed the invasiveness of the cells. In the in vitro invasion assay, Hes1KO PDAC cells showed a significantly higher invasion ability than Hes1WT PDAC cells

(Figure 6*I*). Moreover, we analyzed the influence of *Hes1* deletion on the metastatic property of cells using a murine model of hepatic metastases. After 21 days from splenic injection of PDAC cells, Hes1KO PDAC cells induced larger area of liver metastases compared with Hes1WT PDAC cells (Figure 6*J*). Collectively, these data suggest that *Hes1* suppresses PDAC progression.

## *Hairy and Enhancer of Split-1 Directly Regulates* Muc5ac *Expression by Binding to Its Promoter Region*

To elucidate the mechanism underlying *Hes1* deletion-induced PDAC progression, we performed RNA sequencing (RNA-seq) using the PDAC cell lines described above. RNA was extracted from the 6 PDAC cell lines (Hes1KO #1–3 and Hes1WT #1–3) for RNA-seq (Supplementary Table 2). RNA-seq revealed that 875 genes showed ≥2-fold changes, with either significant up-regulation or down-regulation resulting from Ad-Cre-GFP–mediated *Hes1* deletion (Figure 7*A* and Supplementary Figure 7). Among the significantly up-regulated or down-regulated genes, we focused on the up-regulated genes in Hes1KO cells because HES1 negatively regulates target genes.[7] In the up-regulated genes, *Muc5ac* showed the highest up-regulation by *Hes1* deletion (Figure 7*A*). Among other genes that showed changes in expression patterns in the RNA-seq analysis, several genes that were reportedly associated with pancreatic cancer pathophysiology were up-regulated in Hes1KO cells, including *ITGB6*[27] and *ADAM12.*[28] Gene set enrichment analysis revealed the increased expression of several gene sets in Hes1KO cells, including those involved in the cell cycle and epithelial-to-mesenchymal transition (Figure 7*B* and Supplementary Figure 8*A*). Gene ontology enrichment analysis was performed using the Database for Annotation, Visualization, and Integrated Discovery (DAVID), with 119 genes up-regulated in Hes1KO cells, and several gene ontology biological processes, including positive regulation of cell proliferation, were found to be enriched (Supplementary Figure 8*B*).

Recently, Ganguly et al[29] reported that *Muc5ac* potentiates oncogenic signaling in PanIN mouse models; we predicted that *Hes1* deletion caused *Muc5ac* up-regulation, thereby inducing tumor progression. First, we evaluated mucin 5, subtype AC (MUC5AC) expression in our PDAC mouse model. IHC analysis revealed that MUC5AC expression was higher in Pdx1KP;Hes1KO mice than in Pdx1KP;Hes1WT mice (Figure 7*C*), although not significantly due to the heterogeneity of each tumor (Supplementary Figure 5A). Meanwhile, MUC5AC was also evaluated in the murine hepatic metastasis model, and the difference became clearer (Supplementary Figure 5*C* and *D*). Additionally, the percentage of CK19-positive area in the liver metastasis was higher in Hes1KO PDAC compared with that in Hes1WT PDAC in the metastasis model (Supplementary Figure 5*C*), suggesting tumor density is higher in Hes1KO PDAC than Hes1WT PDAC.

We also evaluated MUC5AC expression in caerulein-induced pancreatitis (Pdx1;Hes1KO and Pdx1;Hes1WT mice) and in PanIN models (Pdx1K;Hes1KO and Pdx1K;Hes1WT mice). In the caerulein-induced pancreatitis model, MUC5AC was not expressed in Pdx1;Hes1KO or Pdx1;Hes1WT mice (Supplementary Figure 2*C*). Conversely, MUC5AC is generally expressed in PanIN, as previously reported,[29] but evaluating its expression in these mice quantitatively by IHC was difficult. In addition, analysis of the pancreatitis-induced PanIN mice model revealed that the pancreatic duct diameter of Pdx1K;Hes1KO in the progression group was larger than that of other groups: Pdx1K;Hes1WT in the progression and initiation group and Pdx1K;Hes1KO in the initiation group (Supplementary Figure 9*A* and *B*). We speculate that in Pdx1K;Hes1KO mice in the progression group, MUC5AC secreted from PanINs might expand the ducts.

Next, we examined whether HES1 directly regulated *Muc5ac* expression. In a previous study, *Muc5ac* was reported to encode N-box, a known target of the HES1 DNA-binding domain, in its promoter region.[30] We performed ChIP using an anti-HES1 antibody. The co-precipitated chromatin DNA fragments extracted from Hes1WT #3 PDAC cells were amplified by PCR using primers for the *Muc5ac* promoter region, including the N-box sequence (Figure 7*D*). As expected, the *Muc5ac* promoter region was also amplified (Figure 7*D*), indicating that HES1 binds to the *Muc5ac* promoter and directly regulates its expression.

We tested whether the effect of *Hes1* deletion on PDAC is attributable to *Muc5ac* up-regulation using small interfering RNA. The efficient loss of *Muc5ac* expression was confirmed by qRT-PCR (Figure 7*E*). The invasion assay demonstrated that the invasion potential of *Muc5ac*-knockdown cells was significantly lower than that of control cells (Figure 7*F*). Additionally, compared with control cells, *Muc5ac*-knockdown cells showed decreased expression of *Vim* and *CD44* mRNA and increased expression of *Cdh1* (Figure 7*G*), which were reported to be regulated by *Muc5ac* in PDAC.[29] These results suggested that the enhancement of PDAC progression in response to *Hes1* depletion is mediated, at least in part, by a *Muc5ac*-dependent mechanism, with the up-regulation of *Vim* and *CD44* and down-regulation of *Cdh1*.

## *Hairy and Enhancer of Split-1 Deletion of Pancreatic Ductal Adenocarcinoma Cells Leads to Squamous Subtype*

PDAC is classified into 2 major groups—the classical/progenitor type and the squamous/basal type—based on the mRNA expression patterns, where enhanced epithelial-to-mesenchymal transition is up-regulated in the squamous/basal type.[6,31,32] In this study, we revealed that Hes1 negatively regulates enhanced epithelial-to-mesenchymal transition in PDAC cells. Therefore, we determined whether the Hes1 expression level is correlated with PDAC subtypes. Gene set enrichment analysis showed that Hes1WT PDAC cells have a progenitor property, whereas Hes1KO PDAC cells have a squamous property (Supplementary Figure 8*C*). We examined whether these results of mice are applicable to human PDAC. Patients with

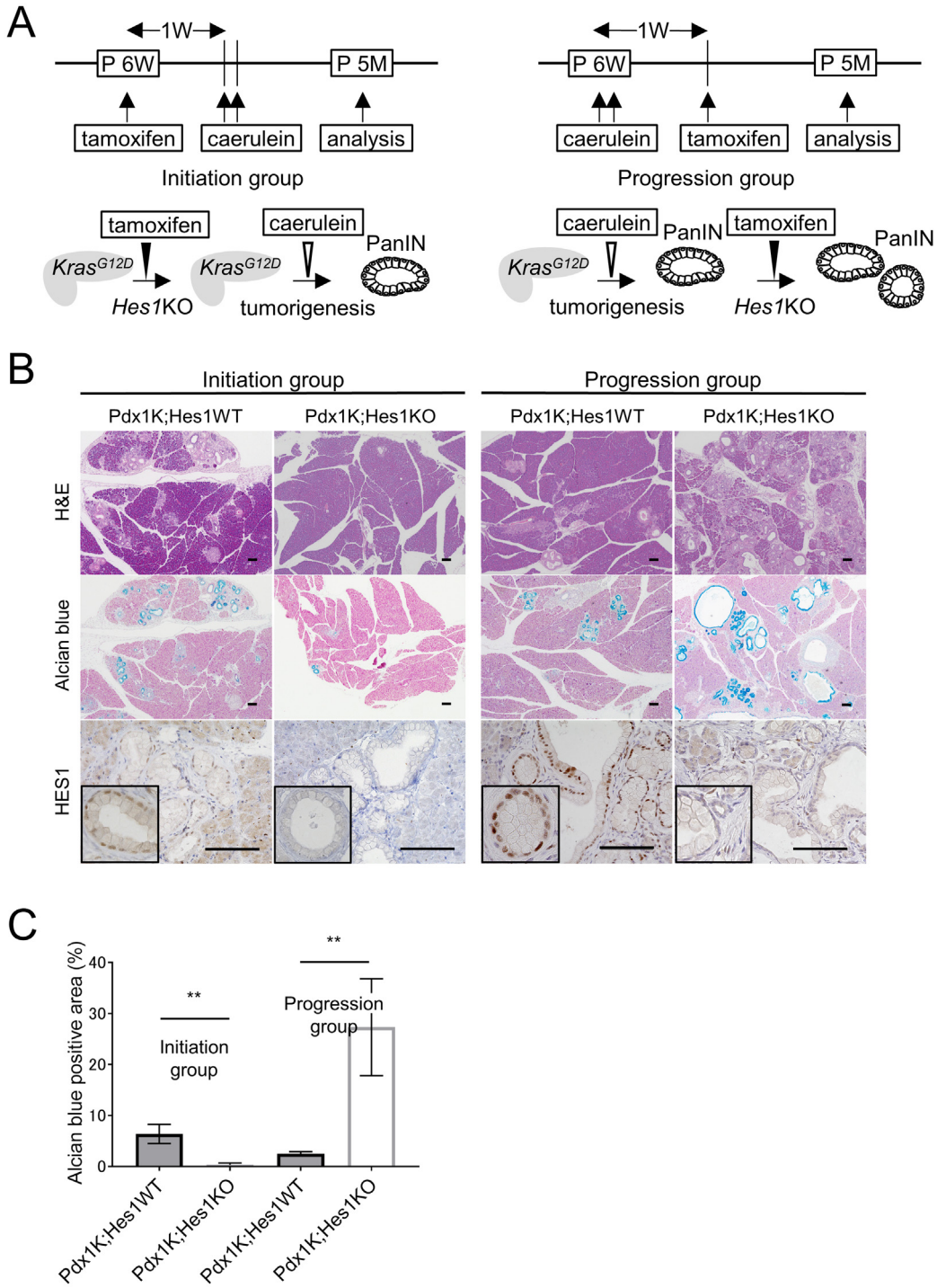


**Figure 5.** HES1 promotes PanIN initiation but inhibits its progression in caerulein-induced pancreatitis. (*A*) Schematic representation of the experimental design for caerulein treatment with tamoxifen administration and analysis. M, month; W, week. (*B*) H&E, Alcian blue, and IHC staining for HES1 in pancreatic tissues of 5-month-old mice. *Scale bars*, 100 $\mu$m. (*C*) Percentage of Alcian blue-positive area in the pancreas (n = 3 in each group). Plotted values represent the mean ± standard deviation. $^{**}P < .01$.

PDAC were divided based on *Hes1* mRNA expression level and analyzed similarly to mouse PDAC. Although progenitor subtype was not associated with the Hes1 expression level, the Hes1-low group showed a squamous property compared with the Hes1-high group (Supplementary Figure 8*D*). Taken together, Hes1 expression level may be correlated with PDAC subtype, and PDACs with low Hes1 expression tend to have squamous phenotype.

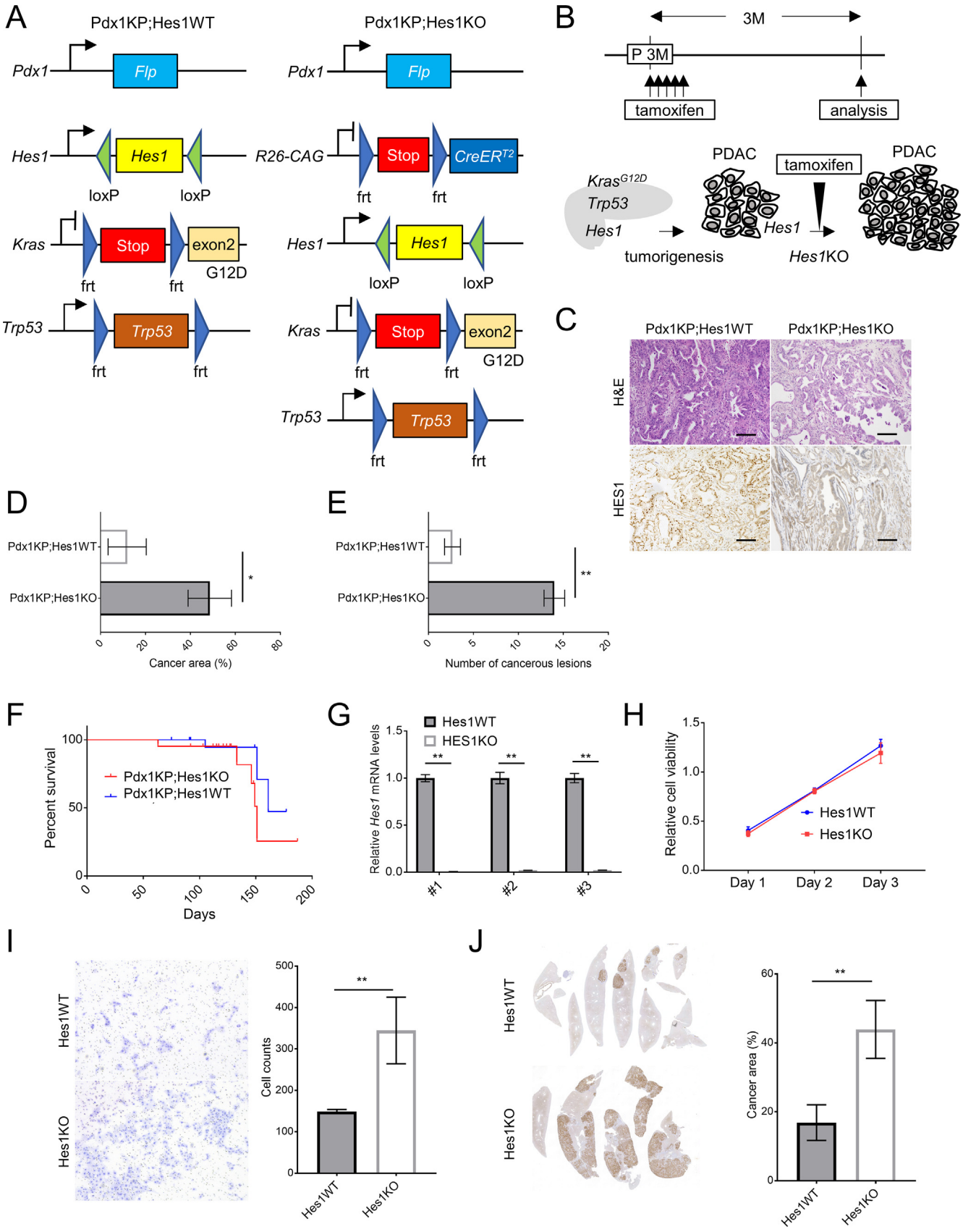
A
Pdx1KP;Hes1WT
Pdx1KP;Hes1KO
Pdx1
Flp
Hes1
loxP
R26-CAG
Stop
CreER^T2
frt
Kras
exon2
G12D
Trp53
B
3M
P 3M
tamoxifen
analysis
PDAC
Kras^G12D
Trp53
Hes1
tumorigenesis
Hes1KO
C
H&E
HES1
D
Cancer area (%)
E
Number of cancerous lesions
F
Percent survival
Days
G
Relative Hes1 mRNA levels
Hes1WT
HES1KO
H
Relative cell viability
Day 1
Day 2
Day 3
I
Cell counts
J
Cancer area (%)

### The Target of Hairy and Enhancer of Split-1 Differs Based on the Tumor Phase

We investigated the reason why *Hes1* deletion has different roles in different phases of the tumor development—tumor initiation and progression. Our previous report[11] and the result of tumor initiation in this study suggest that Hes1 plays an important role in ADM, prelesion of PanIN; therefore, we performed acinar cell culture to elucidate the role of Hes1 in ADM, the first important step of pancreatic tumorigenesis. *Kras*-mutated acinar cells were harvested from 8-week-old *Pdx1-Flp;FSF-Kras$^{G12D}$;Hes$^{1flox/flox}$* mice, digested, and infected with Ad-Cre-GFP or Ad-GFP. After a 24-hour incubation with the adenoviruses, cells were washed and cultured for 2 days, and transcriptome analysis was performed (Supplementary Table 3). We compared RNA-seq data of cultured acinar cells and PDAC cells, described in Supplementary Table 2 and Figure 7. As a result, *Muc5ac* was commonly up-regulated in Hes1KO cultured acinar cells and Hes1KO PDAC cells. However, the enriched pathways were different between Hes1KO cultured acinar cells and Hes1KO PDAC cells, and only 6 and 9 genes were commonly up-regulated and down-regulated, respectively, in both Hes1KO cultured acinar cells and Hes1KO PDAC cells (Supplementary Figure 10*A*–*C*). These differences in Hes1 target genes between cultured acinar cells and PDAC cells might lead to different effects of *Hes1* deletion in the initiation phase vs progression phase stages of pancreatic tumor development.

## Discussion

HES1 is reported to play important roles not only in the maintenance of homeostasis in adult pancreatic cells but also in pancreatic tumorigenesis. However, because HES1 exhibits divergent roles depending on the developmental stage (eg, embryonic or adult stage) and cell type, elucidating its precise function at specific time points and in specific cell types is often difficult. In this study, using a dual-recombinase mouse model, we showed that although HES1 does not play a major role in maintaining pancreatic homeostasis, it is essential in regeneration in centroacinar/terminal duct cells after acute pancreatitis. Moreover, we showed that HES1 plays an oncogenic role in PanIN initiation, but once the process of PanIN development is completed, HES1 exerts a tumor-suppressive function. Our data demonstrated the context-dependent roles of HES1 in the adult pancreas as well as in pancreatic tumor formation.

In the normal pancreas, Hidalgo-Sastre et al[15] and Kuriyama et al[23] independently reported using *Ptf1a-Cre;Hes1$^{flox/flox}$* or *Pdx1-Cre;Hes1$^{flox/flox}$* mice that the loss of *Hes1* expression in fetal pancreatic cells led to normal pancreatic development at birth but induced pancreatic atrophy a few months after birth. In the present study, we used *Pdx1-Flp;FSF-R26$^{CAG-CreERT2}$;Hes1$^{flox/flox}$* mice. We induced *Hes1* deletion in adult pancreatic cells, but no change was observed in the pancreatic morphology for up to 6 months after *Hes1* deletion. Therefore, HES1 was considered to be essential for neonatal pancreatic cell development but dispensable for the maintenance of adult pancreatic cells under normal conditions. Interestingly, we found that once pancreatitis was induced, *Hes1* deletion in adult pancreatic cells impaired exocrine tissue regeneration, which was accompanied by enhanced apoptosis of the pancreatic cells, indicating the involvement of HES1 in regeneration after pancreatic injury. Our data are in agreement with those reported by Hidalgo-Sastre et al,[15] who observed compromised regeneration, ductal metaplasia, and fibrosis with severe acinar atrophy after pancreatitis caused by *Hes1* deletion.

We previously reported that *Hes1* deletion in adult acinar cells did not affect pancreatic regeneration after acute pancreatitis,[11] which contradicts our findings in the present study. The difference in the findings between our previous and present study may be attributed to the difference in the cell types in which *Hes1* deletion was induced. In this study, *Hes1* deletion was induced in all pancreatic cells, whereas in our previous study, *Hes1* deletion was induced only in acinar cells. From these data, it is reasonable to consider that HES1 expression in duct cells or centroacinar/terminal duct cells is important for pancreatic regeneration after pancreatitis. However, we also showed that *Hes1* deletion in duct cells did not affect pancreatic tissue regeneration after pancreatitis.

Previous studies have shown that centroacinar/terminal duct cells play an important role in pancreatic tissue regeneration.[23,33] Accordingly, we attempted to examine the effect of *Hes1* deletion in centroacinar/terminal duct cells in vivo; however, we were unable to do so, because

PANCREAS

**Figure 6.** *Hes1* suppresses PDAC progression. (*A*) Genetic strategy for *Hes1* deletion after PDAC formation in a mouse model in which the activation of oncogenic *Kras$^{G12D}$* with the monoallelic inactivation of *Trp53* was induced in the whole pancreas in Pdx1KP;Hes1WT (control) and Pdx1KP;Hes1KO mice. (*B*) Schematic representation of the experimental design for tamoxifen administration and analysis. M, month. (*C*) H&E and IHC staining for HES1 in the pancreatic tissues of Pdx1KP;Hes1KO and control mice at 3 months after tamoxifen administration. *Scale bars*, 100 $\mu$m. (*D*) Percentage of area with PDAC in the pancreas (n = 8, Pdx1KP;Hes1WT; n = 5, Pdx1KP;Hes1KO). (*E*) Average number of PDACs in representative specimen sections of the pancreas from each mouse (n = 3 in each group). (*F*) Survival analysis of Pdx1KP;Hes1WT and Pdx1KP;Hes1KO mice (n = 15, in each group). (*G*) Analysis by qRT-PCR of *Hes1* mRNA in Hes1WT and Hes1KO PDAC cells that were established from the tumors of 3 *Pdx1-Flp;FSF-Kras$^{G12D}$;Trp53$^{frt/+}$;Hes1$^{flox/flox}$* mice. (*H*) Cell proliferation assay with MTS (3-(4,5-dimethylthiazol-2-yl)-5-(3-carboxymethoxyphenyl)-2-(4-sulfophenyl)-2H-tetrazolium) of Hes1WT and Hes1KO PDAC cell lines (average data of Hes1WT #1–3 and Hes1KO #1–3 were used, respectively). (*I*) Invasion assay (*left*) and quantification of invasion ability (*right*) of Hes1WT and Hes1KO PDAC cell lines (average data of Hes1WT #1–3 and Hes1KO #1–3 were used, respectively). (*J*) Liver metastasis model established by splenic injection of PDAC cell lines. (*Left*), Liver tissues were stained with CK19; the *right panel* shows the analysis of tumor occupying rate (tumor area/whole tissue area × 100) in each section of liver tissues. Plotted values represent the mean ± standard deviation. *$P < .05$; **$P < .01$.

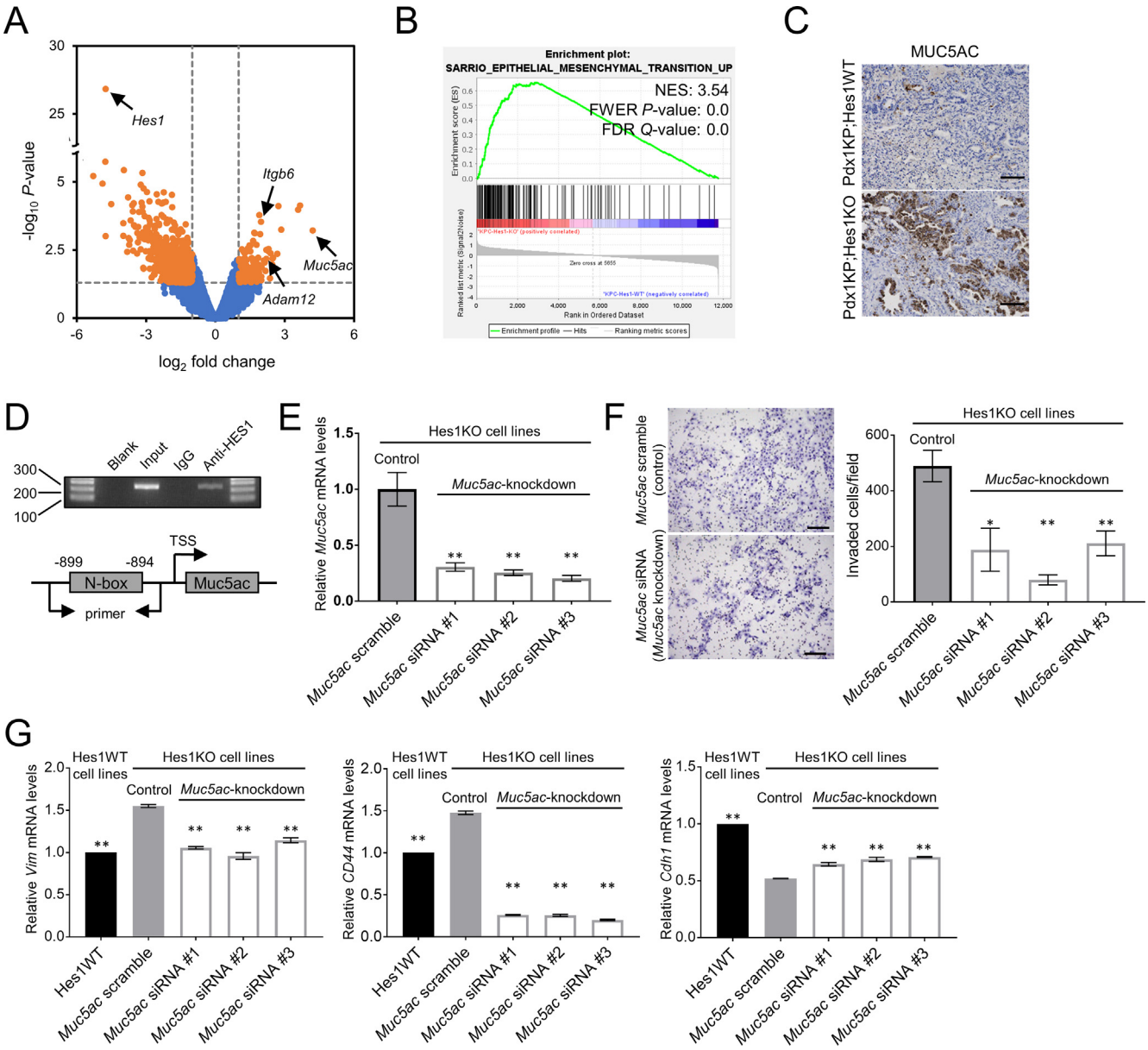


**Figure 7.** HES1 directly regulates *Muc5ac* expression by binding to its promoter region. (*A*) Volcano plot of the differentially expressed genes between Hes1KO and Hes1WT PDAC cells. Significantly down-regulated or up-regulated genes are indicated in *orange*, and genes with nonsignificant changes in expression are indicated in *blue*. The *black vertical dashed lines* highlight $\log_2$ fold changes of $-1$ and 1, and the *black horizontal dashed line* represents a *P* value of .05. (*B*) Gene set enrichment analysis showing significantly up-regulated gene sets in Hes1KO PDAC cells compared with those in Hes1WT PDAC cells. FDR, false discovery rate; FWER, family-wise error rate; NES, normalized enrichment score. (*C*) Pancreatic tissues collected from Pdx1KP;Hes1KO and control mice at 3 months after tamoxifen administration were evaluated using IHC staining for MUC5AC. *Scale bars*, 100 $\mu$m. (*D*) Schematic illustration shows the promoter lesion of *Muc5ac*, N-box, and PCR primer sets. Chromatin preparations from Hes1KO #3 PDAC cells were immunoprecipitated using an anti-HES1 antibody, and co-precipitated DNA fragments were amplified using primers specific for the N-box fragment of the *Muc5ac* promoter. TSS, transcription start site. (*E*) Analysis by qRT-PCR of *Muc5ac* mRNA in Hes1KO PDAC cells (control) and *Muc5ac*-knockdown Hes1KO PDAC cells (n = 3 in each group). siRNA, small interfering RNA. $^{**}P < .01$ vs control). (*F*) Invasion assay and quantification of invasion ability of Hes1KO #3 PDAC cells (control) and *Muc5ac*-knockdown Hes1KO PDAC cells with *Muc5ac* small interfering RNA #1-3 (*Muc5ac*-knockdown) (n = 3 in each group). *Scale bars*, 200 $\mu$m. $^{*}P < .05$ vs control and $^{**}P < .01$ vs control. (*G*) Analysis by qRT-PCR of *Vim*, *Cdh1*, and *CD44* in Hes1WT #3 (Hes1WT), Hes1KO #3 (control), and *Muc5ac*-knockdown in Hes1 KO #3 cells with *Muc5ac* small interfering RNA #1–3 (n = 3 in each group). Plotted values represent the mean ± standard deviation. $^{*}P < .05$ and $^{**}P < .01$ vs control.

centroacinar/terminal duct cell-specific CreERT2 mice were unavailable. To overcome this challenge, we isolated and cultured centroacinar/terminal duct cells using the organoid technique and induced in vitro *Hes1* deletion. We found that *Hes1*-deleted centroacinar/terminal duct cells showed impaired organoid formation, suggesting that HES1

plays an important role in centroacinar/terminal duct cells during pancreatic regeneration after pancreatitis.

In addition to its roles in normal pancreatic development and regeneration, HES1 has been reported to undergo upregulation in PDAC and promote PDAC progression.[34–36] We previously showed that *Hes1* deletion in adult acinar cells suppressed $Kras^{G12D}$-induced tumor formation.[11] However, HES1 expression has been observed not only in PDAC but also in PanIN and ADM.[8,10,14] This may suggest the divergent roles of HES1 in pancreatic tumorigenesis, depending on the stage of progression. Therefore, we induced *Hes1* deletion before and after *Kras*-induced PanIN formation in whole pancreatic cells. Interestingly, although PanIN formation was inhibited when *Hes1* deletion was induced before PanIN formation, it was enhanced when *Hes1* deletion was induced after PanIN formation. Furthermore, we observed that *Hes1* KO promoted *Kras*- and mutant *p53*-induced PDAC formation.

The major difference between the findings from our previous study and those from the present study on PanIN/PDAC formation is the timing of *Hes1* deletion. In the previous study, *Hes1* deletion was performed simultaneously with *Kras* induction,[11,15] whereas in this study, *Hes1* deletion was induced after PanIN/PDAC formation. Collectively, these data strongly suggest that HES1 acts as an accelerator upon tumor initiation and functions as a tumor suppressor during tumor progression. Similar dual functions of pancreatic and duodenal homeobox 1,[37] transforming growth factor-$\beta$,[38] Notch,[39] p21,[40] Kruppel-like factor 4,[40,41] autophagy related 5,[42] and autophagy related 7[43,44] have been reported in pancreatic cancer. In contrast to our present data, HES1 is generally recognized as a tumor promoter in human PDAC, as described above.[34]

Recently, PDAC has been classified 2 two major groups—the classical/progenitor type and the squamous/basal type—based on the mRNA expression patterns.[6,31,32] Classical/progenitor PDAC shows a better prognosis than squamous/basal PDAC. The former is considered to represent an epithelial phenotype, whereas the latter is considered to represent a mesenchymal phenotype. The expression of HES1 was shown to be one of the characteristic factors of classical/progenitor PDAC.[6] Here, we revealed by performing RNA-seq analysis that mouse Hes1WT PDAC has progenitor phenotype and Hes1KO PDAC has squamous phenotype, and Hes1-low human PDAC has squamous subtype.

To elucidate the mechanism underlying PDAC progression induced by *Hes1* deletion, we performed RNA-seq and ChIP-qPCR in PDAC cells isolated from the tumors of *Hes1*-KO mice. Among 875 significantly up-regulated or down-regulated genes, we found *Muc5ac* to be the most significantly up-regulated gene. Interestingly, we revealed that HES1 binds to the *Muc5ac* promoter by using ChIP with an anti-HES1 antibody. These data are compatible with the finding that *Muc5ac* contains the N-box in its promoter region, a known target of the HES1 DNA-binding domain.[30] In addition, we showed that *Muc5ac* knockdown decreased the invasive potential of PDAC cells. Collectively, our data suggest that *Hes1* suppresses PDAC progression, at least in part, through *Muc5ac* regulation with mesenchymal-to-epithelial transition. Although the transcriptome analysis showed that *Muc5ac* was regulated by Hes1 in both cultured acinar cell and PDAC cells, the target genes of Hes1, and the enriched pathways induced by *Hes1* KO differed between PDAC and cultured acinar cells. These data suggest that the distinct roles of Hes1 in the tumor formation might be attributed to the difference of Hes1 target genes at different stages of tumor development; however, further investigations are warranted.

## Conclusion

We demonstrated that HES1 plays an important role in tissue regeneration in pancreatitis. We also showed that HES1 plays different roles, depending on the stage of pancreatic tumor development.

## Supplementary Material

Note: To access the supplementary material accompanying this article, visit the online version of *Gastroenterology* at www.gastrojournal.org, and at https://dx.doi.org/10.1053/j.gastro.2022.08.048.



## References


1. American Cancer Society. Cancer Facts & Figures 2021. Accessed August 1, 2021. https://www.cancer.org/content/dam/cancer-org/research/cancer-facts-and-statistics/annual-cancer-facts-and-figures/2021/cancer-facts-and-figures-2021.pdf.
2. Carioli G, Malvezzi M, Bertuccio P, et al. European cancer mortality predictions for the year 2021 with focus on pancreatic and female lung cancer. Ann Oncol 2021;32:478–487.
3. Vital Statistics Japan, Ministry of Health Labour and Welfare. Cancer Statistics in Japan. Cancer Information Service, National Cancer Center, Japan. Accessed August 1, 2021. https://ganjoho.jp/reg_stat/statistics/dl/index.html.
4. Bardeesy N, DePinho RA. Pancreatic cancer biology and genetics. Nat Rev Cancer 2002;2:897–909.
5. Jemal A, Ward E, Thun M. Declining death rates reflect progress against cancer. PLoS One 2010;5:e9584.
6. Bailey P, Chang DK, Nones K, et al. Genomic analyses identify molecular subtypes of pancreatic cancer. Nature 2016;531:47–52.
7. Kageyama R, Ohtsuka T, Kobayashi T. The Hes gene family: repressors and oscillators that orchestrate embryogenesis. Development 2007;134:1243–1251.
8. Kopinke D, Brailsford M, Shea JE, et al. Lineage tracing reveals the dynamic contribution of Hes1+ cells to the developing and adult pancreas. Development 2011;138:431–441.
9. Jensen J, Pedersen EE, Galante P, et al. Control of endodermal endocrine development by Hes-1. Nat Genet 2000;24:36–44.
10. Miyamoto Y, Maitra A, Ghosh B, et al. Notch mediates TGF$\alpha$-induced changes in epithelial differentiation during pancreatic tumorigenesis. Cancer Cell 2003;3:565–576.

11. Nishikawa Y, Kodama Y, Shiokawa M, et al. Hes1 plays an essential role in Kras-driven pancreatic tumorigenesis. Oncogene 2019;38:4283–4296.
12. Hosokawa S, Furuyama K, Horiguchi M, et al. Impact of Sox9 dosage and Hes1-mediated Notch signaling in controlling the plasticity of adult pancreatic duct cells in mice. Sci Rep 2015;5:8518.
13. Kopp JL, von Figura G, Mayes E, et al. Identification of Sox9-dependent acinar-to-ductal reprogramming as the principal mechanism for initiation of pancreatic ductal adenocarcinoma. Cancer Cell 2012;22:737–750.
14. Hingorani SR, Petricoin EF, Maitra A, et al. Preinvasive and invasive ductal pancreatic cancer and its early detection in the mouse. Cancer Cell 2003;4:437–450.
15. Hidalgo-Sastre A, Brodylo RL, Lubeseder-Martellato C, et al. Hes1 controls exocrine cell plasticity and restricts development of pancreatic ductal adenocarcinoma in a mouse model. Am J Pathol 2016;186:2934–2944.
16. Schönhuber N, Seidler B, Schuck K, et al. A next-generation dual-recombinase system for time-and host-specific targeting of pancreatic cancer. Nat Med 2014; 20:1340–1347.
17. Imayoshi I, Shimogori T, Ohtsuka T, et al. Hes genes and neurogenin regulate non-neural versus neural fate specification in the dorsal telencephalic midline. Development 2008;2541:2531–2541.
18. Jackson EL, Willis N, Mercer K, et al. Analysis of lung tumor initiation and progression using conditional expression of oncogenic K-ras. Genes Dev 2001:3243–3248.
19. Lee C, Moding EJ, Huang X, et al. Generation of primary tumors with Flp recombinase in FRT-flanked p53 mice. Dis Model Mech 2012;402:397–402.
20. Solar M, Cardalda C, Houbracken I, et al. Pancreatic exocrine duct cells give rise to insulin-producing $\beta$ cells during embryogenesis but not after birth. Dev Cell 2009; 17:849–860.
21. Ito T, Udaka N, Yazawa T, et al. Basic helix-loop-helix transcription factors regulate the neuroendocrine differentiation of fetal mouse pulmonary epithelium. Development 2000;127:3913–3921.
22. Mameishvili E, Serafimidis I, Iwaszkiewicz S, et al. Aldh1b1 expression defines progenitor cells in the adult pancreas and is required for Kras-induced pancreatic cancer. Proc Natl Acad Sci U S A 2019;116:20679–20688.
23. Kuriyama K, Kodama Y, Shiokawa M, et al. Essential role of Notch/Hes1 signaling in postnatal pancreatic exocrine development. J Gastroenterol 2021;56:673–687.
24. Cleveland MH, Sawyer JM, Afelik S, et al. Exocrine ontogenies: on the development of pancreatic acinar, ductal and centroacinar cells. Semin Cell Dev Biol 2012; 23:711–719.
25. Guerra C, Collado M, Navas C, et al. Pancreatitis-induced inflammation contributes to pancreatic cancer by inhibiting oncogene-induced senescence. Cancer Cell 2011;19:728–739.
26. McAllister F, Bailey JM, Alsina J, et al. Oncogenic Kras activates a hematopoietic-to-epithelial IL-17 signaling axis in preinvasive pancreatic neoplasia. Cancer Cell 2014;25:621–637.
27. Reader CS, Vallath S, Steele CW, et al. The integrin $\alpha$v$\beta$6 drives pancreatic cancer through diverse mechanisms and represents an effective target for therapy. J Pathol 2019;249:332–342.
28. Veenstra VL, Damhofer H, Waasdorp C, et al. ADAM12 is a circulating marker for stromal activation in pancreatic cancer and predicts response to chemotherapy. Oncogenesis 2018;7:87.
29. Ganguly K, Krishn SR, Rachagani S, et al. Secretory mucin 5AC promotes neoplastic progression by augmenting KLF4-mediated pancreatic cancer cell stemness. Cancer Res 2021;81:91–102.
30. Ou-Yang H-F, Wu C-G, Qu S-Y, et al. Notch signaling downregulates MUC5AC expression in airway epithelial cells through Hes1-dependent mechanisms. Respiration 2013;86:341–346.
31. Collisson EA, Sadanandam A, Olson P, et al. Subtypes of pancreatic ductal adenocarcinoma and their differing responses to therapy. Nat Med 2011;17:500–503.
32. Moffitt RA, Marayati R, Flate EL, et al. Virtual microdissection identifies distinct tumor-and stroma-specific subtypes of pancreatic ductal adenocarcinoma. Nat Genet 2015;47:1168–1178.
33. Beer RL, Parsons MJ, Rovira M. Centroacinar cells: at the center of pancreas regeneration. Dev Biol 2016; 413:8–15.
34. Cao F, Li J, Sun H, et al. HES 1 is essential for chemoresistance induced by stellate cells and is associated with poor prognosis in pancreatic cancer. Oncol Rep 2015;33:1883–1889.
35. Liu ZH, Dai XM, Du B. Hes1: a key role in stemness, metastasis and multidrug resistance. Cancer Biol Ther 2015;16:353–359.
36. Rani A, Greenlaw R, Smith RA, et al. HES1 in immunity and cancer. Cytokine Growth Factor Rev 2016; 30:113–117.
37. Roy N, Takeuchi KK, Ruggeri JM, et al. PDX1 dynamically regulates pancreatic ductal adenocarcinoma initiation and maintenance. Genes Dev 2016;30:2669–2683.
38. Siegel PM, Massagué J. Cytostatic and apoptotic actions of TGF-beta in homeostasis and cancer. Nat Rev Cancer 2003;3:807–821.
39. Radtke F, Raj K. The role of Notch in tumorigenesis: oncogene or tumour suppressor? Nat Rev Cancer 2003; 3:756–767.
40. Rowland BD, Peeper DS. KLF4, p21 and context-dependent opposing forces in cancer. Nat Rev Cancer 2006;6:11–23.
41. Maddipati R, Katz JP. KLF4 initiates acinar cell reprogramming and is essential for the early stages of pancreatic carcinogenesis. Cancer Cell 2016; 29:247–248.
42. Rao S, Tortola L, Perlot T, et al. A dual role for autophagy in a murine model of lung cancer. Nat Commun 2014; 5:3056.
43. Takamura A, Komatsu M, Hara T, et al. Autophagy-deficient mice develop multiple liver tumors. Genes Dev 2011;25:795–800.
44. Lévy J, Cacheux W, Bara MA, et al. Intestinal inhibition of Atg7 prevents tumour initiation through a microbiome-

influenced immune response and suppresses tumour growth. Nat Cell Biol 2015;17:1062–1073.

**Received November 26, 2021. Accepted August 30, 2022.**

**Correspondence**
Address correspondence to: Masahiro Shiokawa, MD, PhD, Department of Gastroenterology and Hepatology, Kyoto University Graduate School of Medicine, 54 Kawahara-cho, Shogoin, Sakyo-ku, Kyoto 606-8507, Japan. e-mail: machan@kuhp.kyoto-u.ac.jp.

**Acknowledgments**
The authors thank Yuta Kawamata and Taichi Ito for their extensive technical support. Saiko Marui amd Yoshihiro Nishikawa contributed equally.

**CRediT Authorship Contributions**
Saiko Marui, MD (Conceptualization: Equal; Investigation: Equal; Writing – original draft: Equal).
Yoshihiro Nishikawa, MD, PhD (Funding acquisition: Supporting; Investigation: Equal; Methodology: Equal; Writing – original draft: Equal).
Masahiro Shiokawa, MD, PhD (Conceptualization: Equal; Supervision: Lead; Writing – review & editing: Lead).
Masataka Yokode, MD (Writing – review & editing: Supporting).
Shimpei Matsumoto, MD (Writing – review & editing: Supporting).
Yuya Muramoto, MD (Writing – review & editing: Supporting).
Sakiko Ota, MD (Writing – review & editing: Supporting).
Takeharu Nakamura, MD (Writing – review & editing: Supporting).
Hiroyuki Yoshida, MD (Writing – review & editing: Supporting).
Hirokazu Okada, MD (Writing – review & editing: Supporting).
Takeshi Kuwada, MD (Writing – review & editing: Supporting).
Tomoaki Matsumori, MD, PhD (Writing – review & editing: Supporting).
Katsutoshi Kuriyama, MD (Writing – review & editing: Supporting).
Akihisa Fukuda, MD, PhD (Writing – review & editing: Supporting).
Dieter Saur, MD, PhD (Writing – review & editing: Supporting).
Takashi Aoi, MD, PhD (Writing – review & editing: Supporting).
Norimitsu Uza, MD, PhD (Writing – review & editing: Supporting).
Yuzo Kodama, MD, PhD (Writing – review & editing: Supporting).
Tsutomu Chiba, MD, PhD (Writing – review & editing: Supporting).
Hiroshi Seno, MD, PhD (Writing – review & editing: Supporting).

**Conflicts of interest**
The authors disclose no conflicts.

**Funding**
This work was supported by the Pancreas Research Foundation of Japan, the Foundation for Promotion of Cancer Research, Japan Society for the Promotion of Science (JSPS) and Ministry of Education, Culture, Sports, Science and Technology (MEXT) Grants-in-Aid for Scientific Research (KAKENHI) (17H06803 and 20J01362), Moonshot Research & Development Program (JPMJMS2022-1), and COI-NEXT (JPMJPF2018).

# Supplementary Methods

## In Vitro Invasion Assay

The in vitro invasion assay was performed using a Corning BioCoat Matrigel Invasion Chamber (Corning, Corning, NY) in 24-well plates according to the manufacturer's instructions. Briefly, pancreatic cancer cells ($1.0 \times 10^5$ cells/well) were seeded with serum-free DMEM in the upper Matrigel-coated membrane with 8-$\mu$m pores. The lower chambers were filled with DMEM supplemented with 10% FBS (Thermo Fisher Scientific). After incubation for 20 hours, the noninvading cells were carefully removed using a cotton swab. Cells that penetrated the Matrigel-coated membrane were fixed with 100% methanol for 10 minutes and then stained with hematoxylin. The number of invading cells was manually counted from the low-power magnification images. The mean score was calculated from 5 images.

## Cell Proliferation Assay

Cell proliferation was evaluated using the Promega Cell Titer 96 Aqueous One Solution (Promega) according to the manufacturer's instructions. The cells were seeded into a well in a 96-well plate ($5.0 \times 10^3$ cells/well) and cultured in 100 $\mu$L of DMEM supplemented with 10% FBS and 1% penicillin/streptomycin antibiotic mixture, and were incubated at 37°C for different durations (24, 48, and 72 hours), and 20 $\mu$L of the 3-(4,5-dimethylthiazol-2-yl)-5-(3-carboxymethoxyphenyl)-2-(4-sulfophenyl)-2H-tetrazolium (MTS) reagent was added. Cells were then incubated for 60 minutes at 37°C. Absorbance was measured at 492 nm using a Sunrise microplate reader (Tecan, Männedorf, Switzerland). At least 3 replicates were prepared for each experiment.

## Acinar Cell Culture

We performed acinar cell culture as previously described,[1] with minor modification. Briefly, the whole pancreas was chopped into small pieces and digested in Hank's balanced salt solution (HBSS; Thermo Fisher Scientific) supplemented with 0.2 mg/mL collagenase P (Sigma-Aldrich) and 2 U/mL RQ1 RNase-Free DNase (Promega) at 37°C for 10 minutes. After 2 washes with HBSS supplemented with 5% FBS, collagenase-digested pancreatic tissue was sequentially filtered through a 100-$\mu$m cell strainer (Corning). The flow through was layered onto HBSS supplemented with 30% FBS and centrifuged. The cellular pellet was resuspended in Waymouth's Media MB 752/1 1× medium (Thermo Fisher Scientific) supplemented with 10% FBS, 1% penicillin/streptomycin antibiotic mixture (Thermo Fisher Scientific), 100 $\mu$g/mL trypsin inhibitor (Sigma-Aldrich), and 1 $\mu$g/mL dexamethasone (Sigma-Aldrich).

For *Hes1* deletion, acinar cells were incubated at 37°C with an Ad-GFP or Ad-Cre-GFP at a multiplicity of infection (MOI) of 300. After incubation for 24 hours with the adenoviruses, acinar cells were washed and cultured in Matrigel for 2 days, and total RNA was extracted for RNA-seq.

## Small Interfering RNA Transfection

For knockdown experiments, mouse *Muc5ac* small interfering (si)RNA and a nontargeting negative control siRNA (ON-TARGET*plus* siRNA; Horizon Discovery, Cambridge, United Kingdom) were used. Cells were plated in 6-well plates. On the following day, mixtures of siRNA and the Lipofectamine RNAiMAX reagent (Thermo Fisher Scientific) were added to each well as 30 nmol/L siRNA solutions. The effectiveness of *Muc5ac* mRNA knockdown was confirmed after 48 h.

## Adenovirus Infection

For *Hes1* deletion in pancreatic organoids and PDAC cell lines, an adenoviral vector was used. For adenoviral infection, pancreatic organoids and PDAC cells were incubated at 37°C with Ad-GFP or Ad-Cre-GFP at a MOI of 300 for 24 h.

## Three-Dimensional Culture of Adult Pancreas Progenitor Organoids

FACS-isolated Aldh-positive cells were seeded in 25 $\mu$L of growth factor-reduced Matrigel (BD Biosciences, San Jose, CA) in a 48-well plate (Corning). After gelation of the Matrigel for 10 minutes at 37°C in an incubator, the culture medium was added. The culture medium was composed of Advanced DMEM/F-12 (Thermo Fisher Scientific) supplemented with 2% B27 (Thermo Fisher Scientific), 1% penicillin/streptomycin, 1 mmol/L HEPES (Thermo Fisher Scientific), 1% Glutamax (Thermo Fisher Scientific), 1.25 mmol/L *N*-acetylcysteine (Sigma-Aldrich), 10 nmol/L gastrin (Sigma-Aldrich), 50 ng/mL epidermal growth factor (PeproTech, Cranbury, NJ), 250 ng/mL RSP01 (R&D Systems, Minneapolis, MN), 100 ng/mL Noggin (PeproTech), 100 ng/mL fibroblast growth factor 10 (PeproTech), 10 mmol/L nicotinamide (Sigma-Aldrich), 500 nmol/L A83-01 (Tocris Bioscience, Bristol, United Kingdom), and 10 $\mu$mol/L Y27632 (Tocris Bioscience). The culture medium was replaced with fresh medium every 3 days. The organoids were first passaged after 10 to 14 days, depending on their growth. After the first passage, the organoids were passaged every 5 to 7 days, depending on their growth. To passage organoids, the Matrigel was dissolved by incubation in TrypLE (Thermo Fisher Scientific) for 10 minutes on a shaker at 37°C. Cells were washed with DMEM, counted, and centrifuged at 300*g* for 3 minutes at 4°C, after which the cell pellet was resuspended and seeded in 25 $\mu$L of growth factor-reduced Matrigel in a 48-well plate.

## Pancreatic Organoid Proliferation Assay

The proliferation of pancreatic organoids was evaluated using PrestoBlue (Thermo Fisher Scientific) according to the manufacturer's instructions. The organoids were dissociated into single cells, and the number of cells was counted. The cells ($1.0 \times 10^5$ cells/well) were infected with adenoviral vectors (Ad-Cre-GFP or Ad-GFP) at an MOI of 300 for 24 hours. After infection, half of the cells were used

for RNA extraction, and the remaining cells were seeded in 5 wells of a 96-well plate.

For the proliferation assay, 90 $\mu$L of the medium supplemented with 10 $\mu$L of the PrestoBlue solution was added to each well, followed by incubation for 1 hour. Absorbance was measured using a microplate reader at 570 nm and 595 nm.

### RNA Isolation and RNA Sequencing

RNA was extracted using the RNeasy RNA Mini Kit (Qiagen, Hilden, Germany). Library construction and sequencing were performed at Macrogen Japan (Tokyo, Japan) using the TruSeq Stranded mRNA Library Prep Kit (Illumina, San Diego, CA) and NovaSeq 6000 (Illumina).

### RNA Sequencing Data Analysis

Gene set enrichment analysis (GSEA) was performed using GSEA 4.1.0 software.[2] To identify the PDAC subtype, the top 500 genes determining the squamous or progenitor subtype were used to generate gene sets, referred to as Squamous-PDA or Progenitor-PDA Identity Signature, respectively, as previously described.[3,4] The Cancer Genome Atlas's Human PDAC RNA-seq data were obtained from the database for human PDAC analysis. To evaluate the relationship between *Hes1* and PDAC subtype, patients with PDAC were equally divided into 3 groups based on *Hes1* expression, namely, "Hes1-high," "Hes1-middle," and "Hes1-low." Hes1-high and Hes1-low groups were used for PDAC subtype analysis. Gene ontology enrichment analysis of the differentially expressed genes data was performed using the Database for Annotation, Visualization, and Integrated Discovery (DAVID) 6.8 software.[5,6]

### Quantitative Reverse-Transcription Polymerase Chain Reaction Analysis

The extracted RNA was used for complementary DNA synthesis via the ReverTra Ace qPCR RT Master Mix (Toyobo, Osaka, Japan) and subjected to qRT-PCR using the SYBR Green Master Mix (Roche). The expression levels of the indicated genes were normalized to that of *GAPDH*, which was used as a housekeeping gene. The relative expression was expressed in terms of fold change ($2^{-\Delta\Delta Ct}$), with the value obtained in the control group set to 1. The primer sequences are provided in Supplementary Table 4. All reactions were performed in triplicate.

### Chromatin Immunoprecipitation-Quantitative Polymerase Chain Reaction

Immunoprecipitation was performed using the SimpleChIP Enzymatic Chromatin IP Kit (Cell Signaling Technology, Danvers, MA), according to the manufacturer's instructions. An HES1 antibody (generously provided by Tetsuo Sudo) was used for immunoprecipitation. In-put DNA or normal rabbit IgG (#2729, Cell Signaling Technology) was used as the control. After ChIP, the DNA was quantified using qPCR with primers specific for the N-box fragment of the *Muc5ac* promoter as follows: 5′-CTGTCTGTCTCTCTGTCTCT-3′ and 5′-CATTT-GAACTTTCTGGTTGC-3′.

### H Score

The expression of Hes1 and MUC5AC in tumor cells was assessed using the H score,[7] calculated by multiplying the intensity (0, 1, 2, and 3) by the extent of each staining intensity (%). The definition of intensity of staining was as follows: 0, no expression; 1, weak expression; 2, moderate expression; 3, strong expression.

## Supplementary References


1. Means AL, Meszoely IM, Suzuki K, et al. Pancreatic epithelial plasticity mediated by acinar cell transdifferentiation and generation of nestin-positive intermediates. Development 2005;132:3767–3776.
2. Subramanian A, Tamayo P, Mootha VK, et al. Gene set enrichment analysis: a knowledge-based approach for interpreting genome-wide expression profiles. Proc Natl Acad Sci U S A 2005;102:15545–15550.
3. Bailey P, Chang DK, Nones K, et al. Genomic analyses identify molecular subtypes of pancreatic cancer. Nature 2016;531:47–52.
4. Yuan TL, Amzallag A, Bagni R, et al. Differential effector engagement by oncogenic KRAS. Cell Rep 2018; 22:1889–1902.
5. Huang DW, Sherman BT, Lempicki RA. Systematic and integrative analysis of large gene lists using DAVID bioinformatics resources. Nat Protoc 2008;4:44–57.
6. Huang DW, Sherman BT, Lempicki RA. Bioinformatics enrichment tools: paths toward the comprehensive functional analysis of large gene lists. Nucleic Acids Res 2009;37:1–13.
7. Jensen K, Krusenstjerna-Hafstrøm R, Lohse J, et al. A novel quantitative immunohistochemistry method for precise protein measurements directly in formalin-fixed, paraffin-embedded specimens: analytical performance measuring HER2. Mod Pathol 2017; 30:180–193.

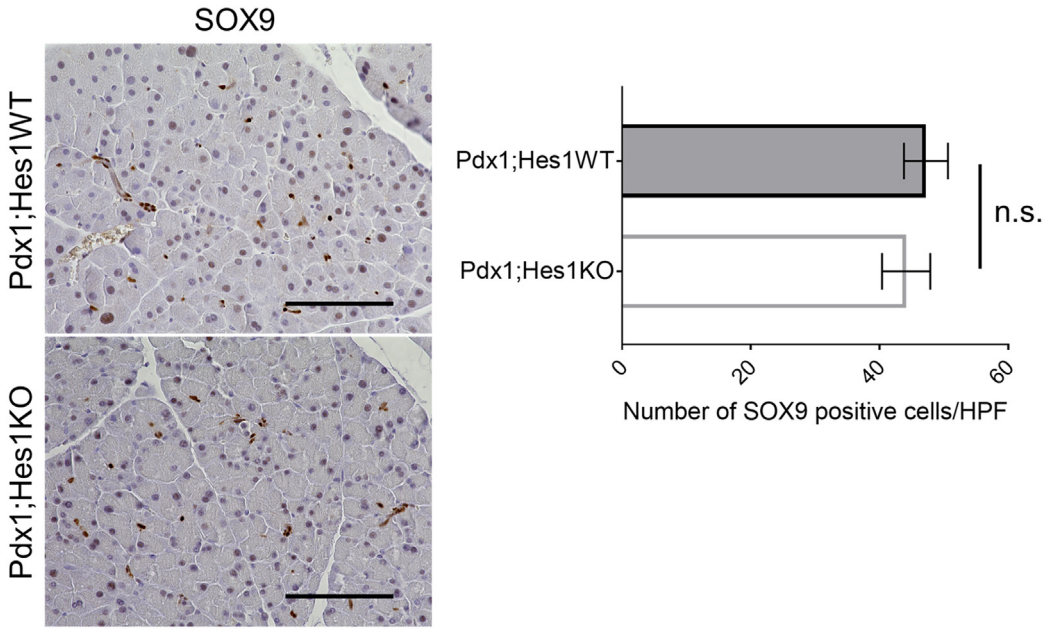


**Supplementary Figure 1.** IHC staining for SOX9 (sex determining region Y-box transcription factor 9) of adult Pdx1;Hes1WT and Pdx1;Hes1KO mice (*left*). Quantitative analysis of SOX9-positive cells (*right*). Five high power fields (HPF) from each group ($n = 3$) were randomly selected, and the number of SOX9-positive cells in the peripheral acinar cells, which did not include main/interlobular duct cells, was counted for each field. *Scale bars,* 100 $\mu$m. Plotted values represent the mean $\pm$ standard deviation. n.s., not significant.

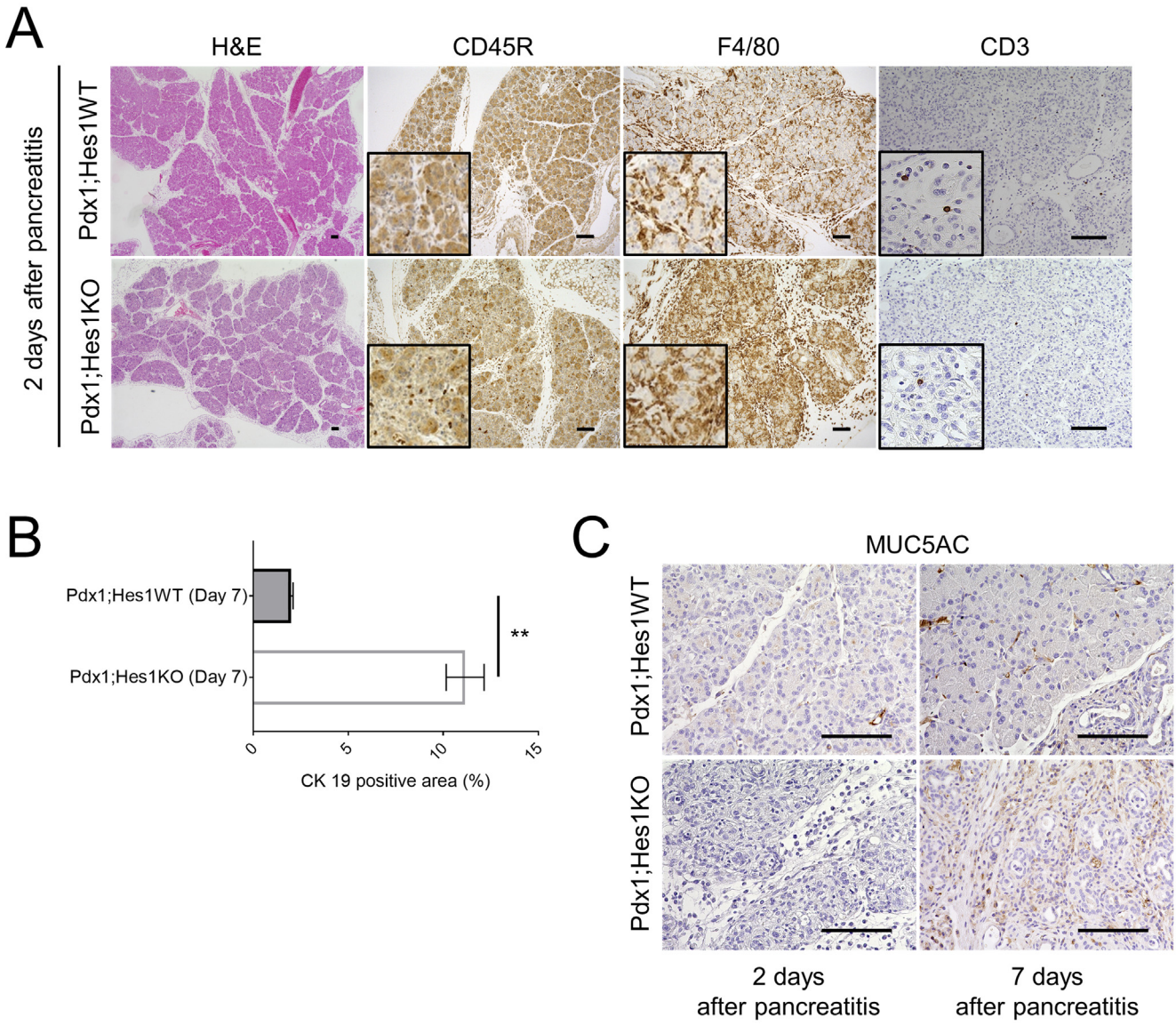


**Supplementary Figure 2.** (*A*) IHC staining for CD45R, F4/80, and CD3 shows infiltration of inflammatory cells in the pancreas of Pdx1;Hes1WT and Pdx1;Hes1KO mice at 2 days after pancreatitis. H&E staining shows diffuse expansion of interlobular septa in both Pdx1;Hes1WT and Pdx1;Hes1KO mice 2 days after pancreatitis. (*B*) Percentage of CK19-positive area in the pancreas (n = 3 in each group). (*C*) IHC staining for MUC5AC in pancreatic tissues at 2 and 7 days after caerulein-induced acute pancreatitis. *Scale bars*, 100 $\mu$m. Plotted values represent the mean ± standard deviation. $^{**}P < .01$.

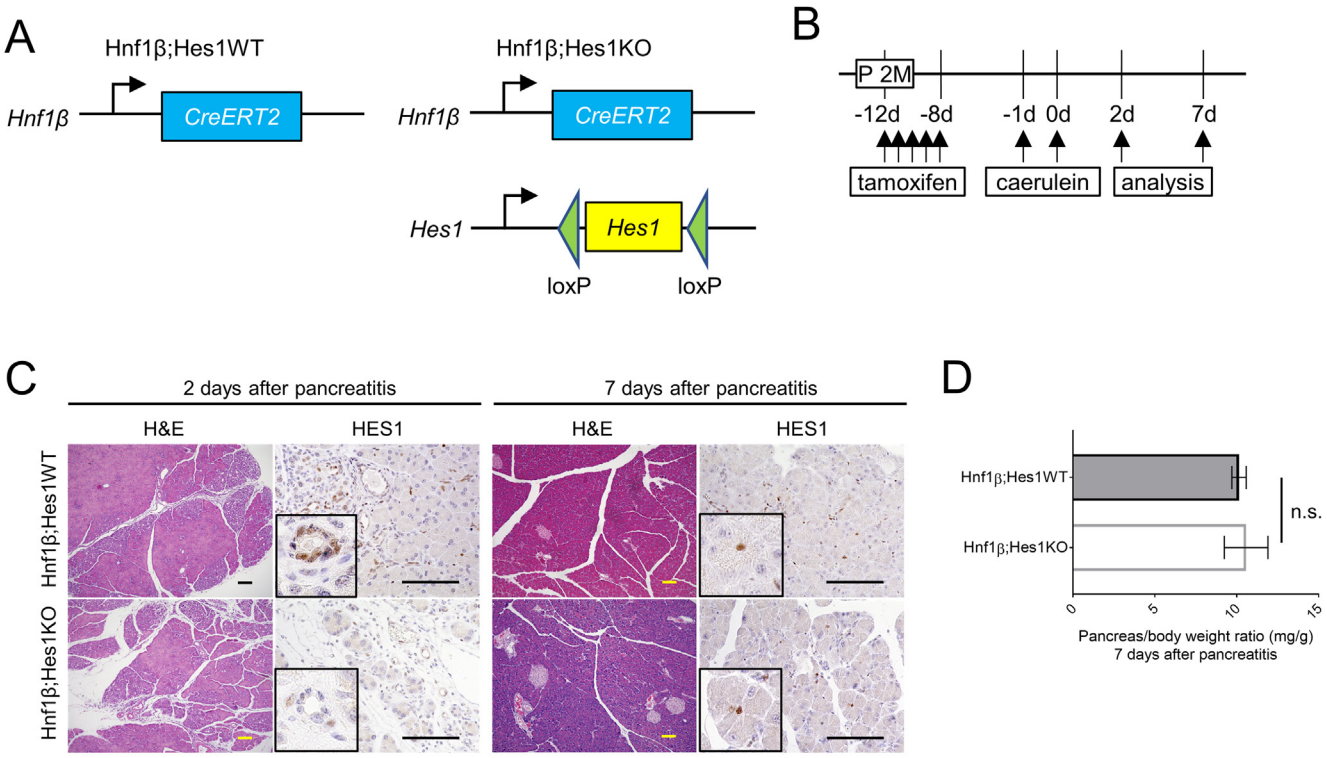


**Supplementary Figure 3.** (*A*) Strategy for *Hes1* deletion in adult duct cells via time-specific tamoxifen-mediated CreERT2 activation. *Hnf1β-CreERT2* mice (Hnf1β;Hes1WT) and *Hnf1β-CreERT2;Hes1*$^{flox/flox}$ mice (Hnf1β;Hes1KO) are shown. (*B*) Schematic presentation of the experimental design for tamoxifen administration, caerulein-induced acute pancreatitis, and analysis. d, day; M, month. (*C*) H&E staining and IHC for HES1 at 2 and 7 days after caerulein-induced acute pancreatitis. (*D*) Ratio of pancreas weight to body weight in Hnf1β;Hes1WT (n = 6) and Hnf1β;Hes1KO (n = 4) mice at 7 days after caerulein-induced acute pancreatitis. *Scale bars*, 100 μm. Plotted values represent the mean ± standard deviation. n.s., not significant.

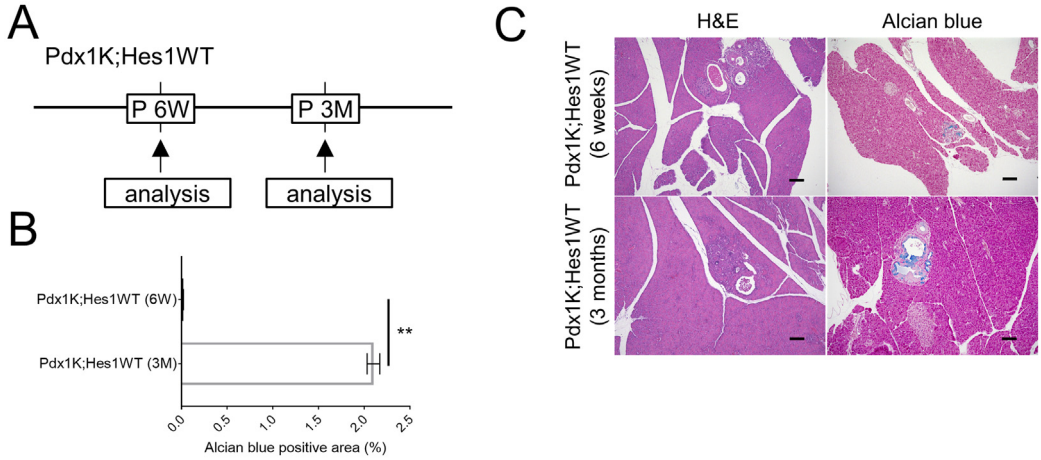


**Supplementary Figure 4.** (*A*) Schematic representation of the experimental design for caerulein treatment and analyses. M, month; W, week. (*B*) Percentage of Alcian blue-positive area in the pancreas (n = 3 in each group). Plotted values represent the mean ± standard deviation. $^{**}P < .01$. (*C*) H&E, Alcian blue, and IHC staining for HES1 in pancreatic tissues. *Scale bars*, 100 μm.

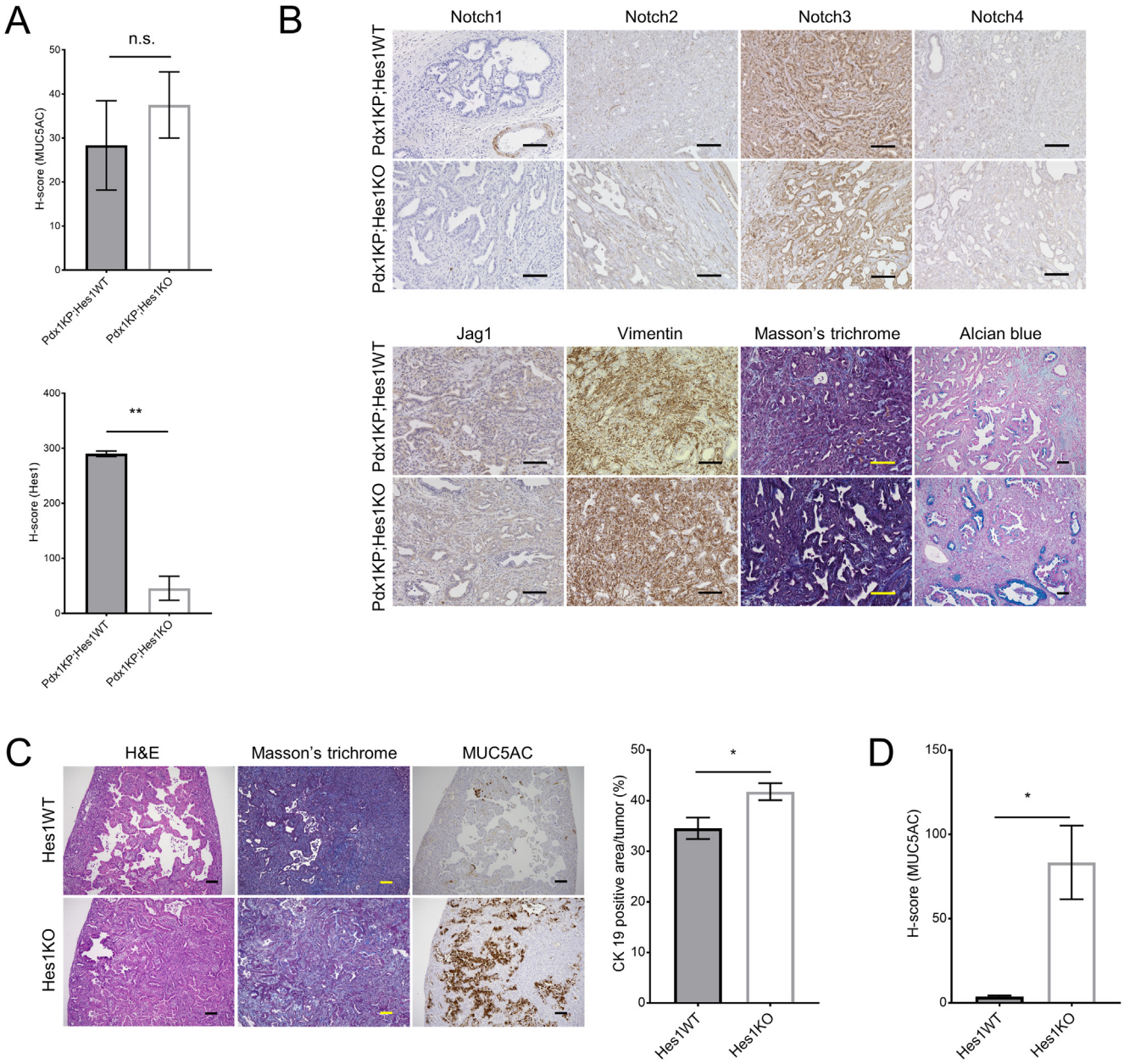


**Supplementary Figure 5.** (*A*) H-score of HES1 and MUC5AC in PDAC of Pdx1KP;Hes1WT and Pdx1KP;Hes1KO mice (n = 3 in each group). (*B*) IHC staining for Notch1, Notch2, Notch3, Notch4, Jag1, and vimentin, and Masson's trichrome and Alcian blue staining in the pancreatic tissues of Pdx1KP;Hes1WT and Pdx1KP;Hes1KO mice at 3 months after tamoxifen administration. (*C*) H&E, Masson's trichrome staining, and IHC staining for MUC5AC of murine model of hepatic metastases. The *right graph* shows the percentage of the CK19-positive area in the hepatic metastasis. *Scale bars*, 100 $\mu$m. (*D*) H-score of MUC5AC for the hepatic metastasis model with Hes1WT and Hes1KO PDAC cells (n = 3 in each group). Plotted values represent the mean ± standard deviation. n.s., not significant; **P* < .05; ***P* < .01.

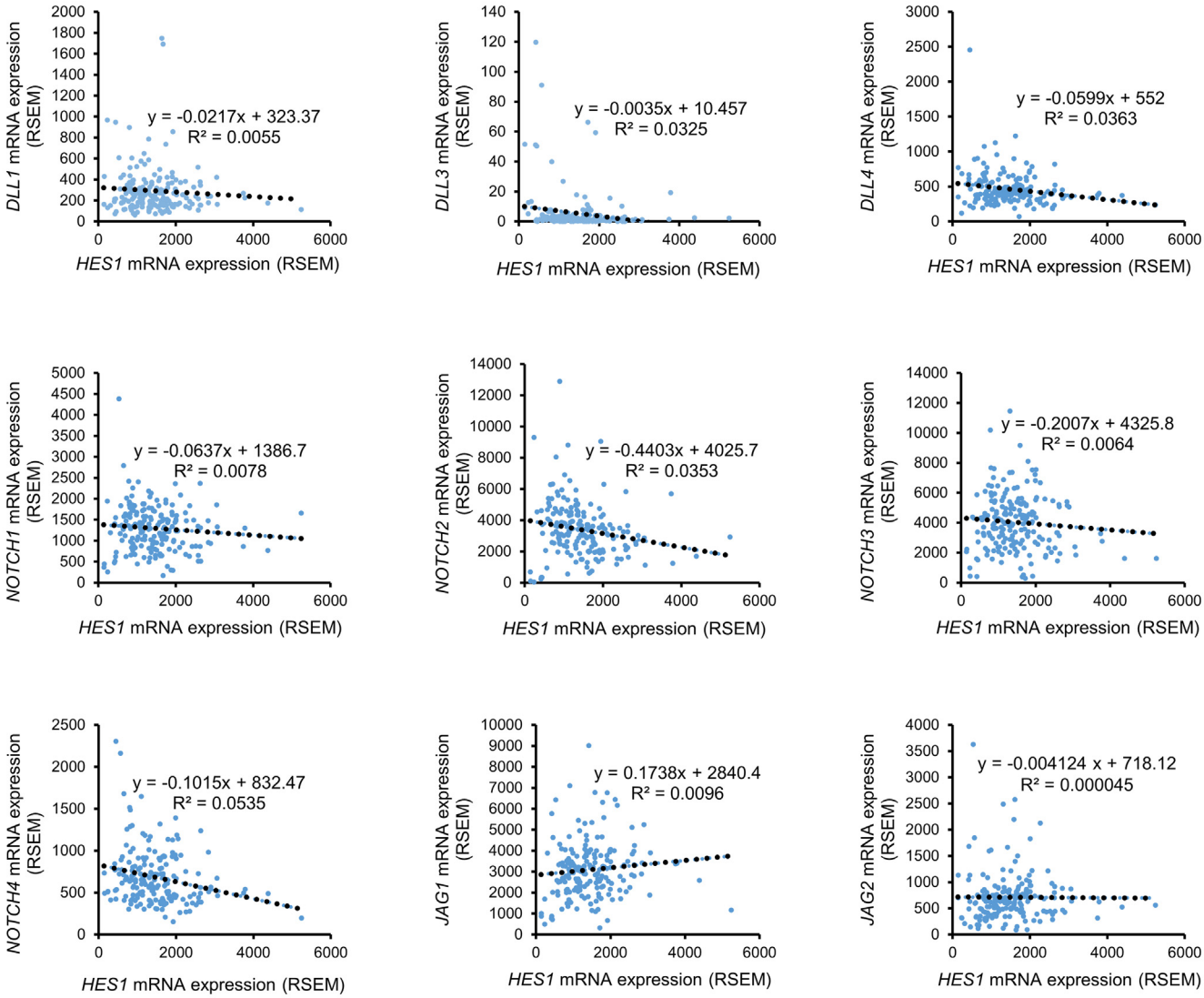


**Supplementary Figure 6.** Correlation between mRNA expression of *Hes1* and *Notch* ligands and receptors in human pancreatic cancer using The Cancer Genome Atlas pancreatic cancer database. RSEM, RNA-seq by expectation maximization.

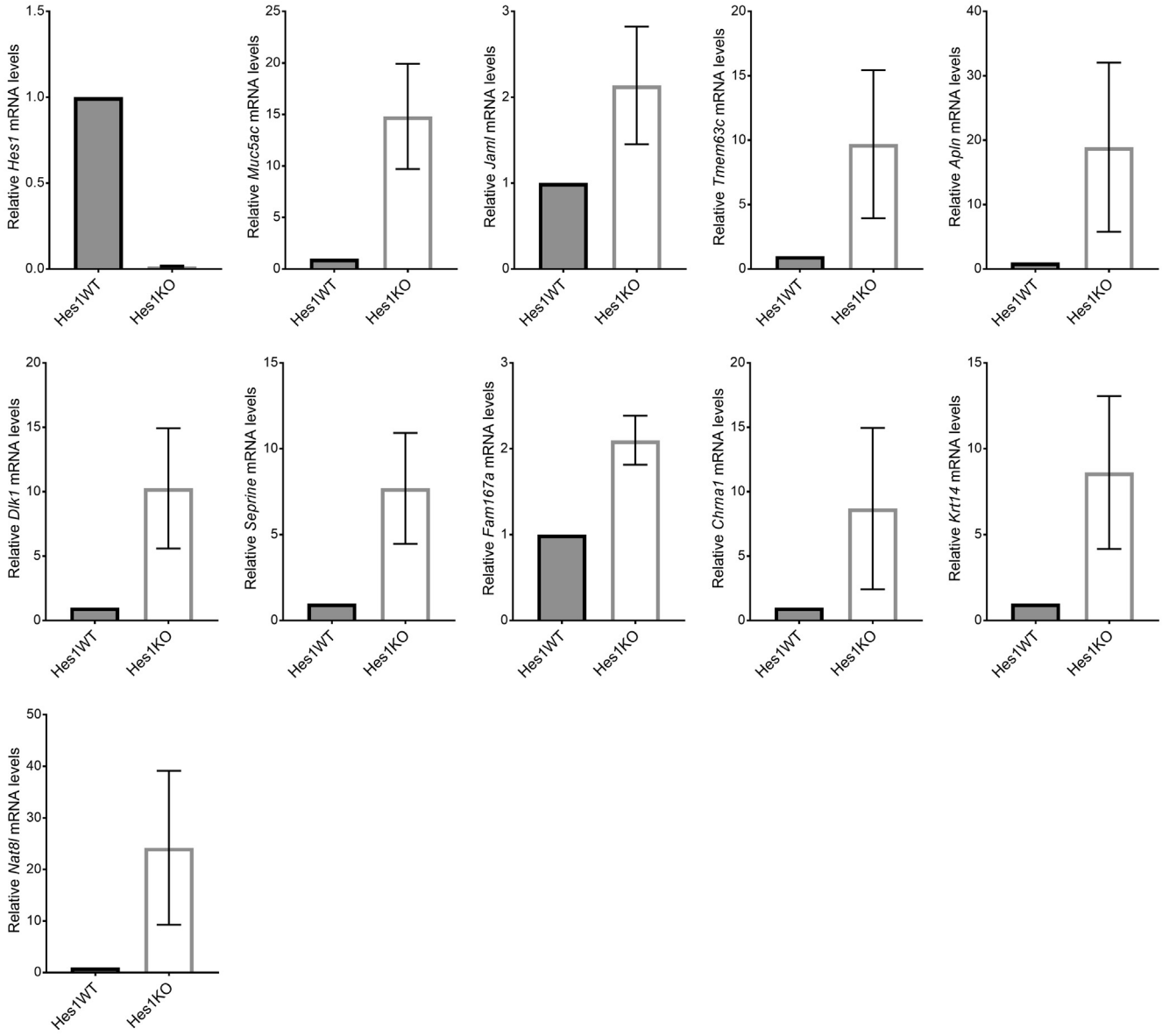


**Supplementary Figure 7.** Validation of mRNA expression in Hes1 (*top left*) and the top 10 genes of differentially expressed genes between Hes1KO and Hes1WT PDAC cells (n = 3 in each group). Plotted values represent the mean ± standard deviation.

A

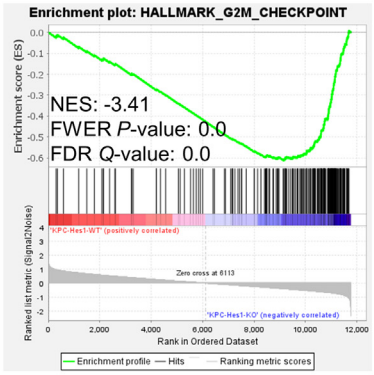
Enrichment plot: HALLMARK_G2M_CHECKPOINT
NES: -3.41
FWER P-value: 0.0
FDR Q-value: 0.0
Enrichment score (ES)
Ranked list metric (Signal2Noise)
'KPC-Hes1-WT' (positively correlated)
Zero cross at 6113
'KPC-Hes1-KO' (negatively correlated)
Rank in Ordered Dataset
Enrichment profile
Hits
Ranking metric scores

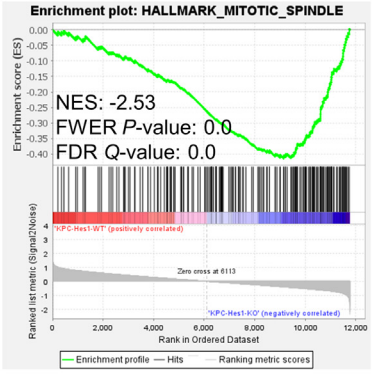
Enrichment plot: HALLMARK_MITOTIC_SPINDLE
NES: -2.53
FWER P-value: 0.0
FDR Q-value: 0.0
Enrichment score (ES)
Ranked list metric (Signal2Noise)
'KPC-Hes1-WT' (positively correlated)
Zero cross at 6113
'KPC-Hes1-KO' (negatively correlated)
Rank in Ordered Dataset
Enrichment profile
Hits
Ranking metric scores

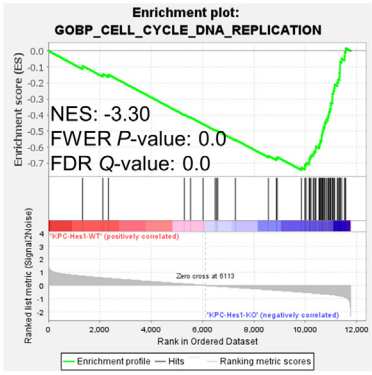
Enrichment plot:
GOBP_CELL_CYCLE_DNA_REPLICATION
NES: -3.30
FWER P-value: 0.0
FDR Q-value: 0.0
Enrichment score (ES)
Ranked list metric (Signal2Noise)
'KPC-Hes1-WT' (positively correlated)
Zero cross at 6113
'KPC-Hes1-KO' (negatively correlated)
Rank in Ordered Dataset
Enrichment profile
Hits
Ranking metric scores

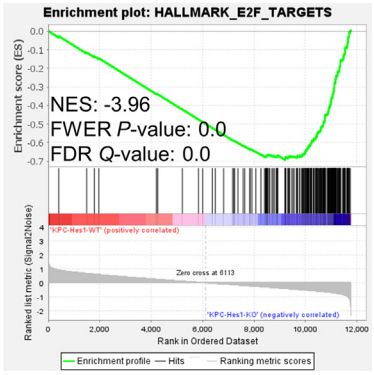
Enrichment plot: HALLMARK_E2F_TARGETS
NES: -3.96
FWER P-value: 0.0
FDR Q-value: 0.0
Enrichment score (ES)
Ranked list metric (Signal2Noise)
'KPC-Hes1-WT' (positively correlated)
Zero cross at 6113
'KPC-Hes1-KO' (negatively correlated)
Rank in Ordered Dataset
Enrichment profile
Hits
Ranking metric scores

B

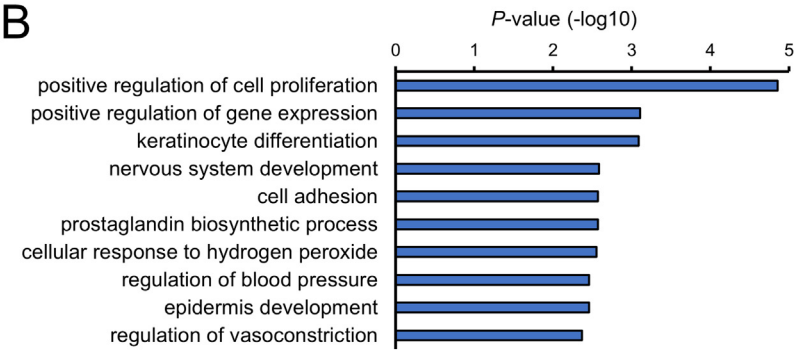
P-value (-log10)
0
1
2
3
4
5
positive regulation of cell proliferation
positive regulation of gene expression
keratinocyte differentiation
nervous system development
cell adhesion
prostaglandin biosynthetic process
cellular response to hydrogen peroxide
regulation of blood pressure
epidermis development
regulation of vasoconstriction

C

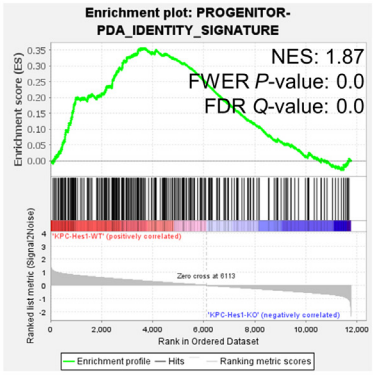
Enrichment plot: PROGENITOR-
PDA_IDENTITY_SIGNATURE
NES: 1.87
FWER P-value: 0.0
FDR Q-value: 0.0
Enrichment score (ES)
Ranked list metric (Signal2Noise)
'KPC-Hes1-WT' (positively correlated)
Zero cross at 6113
'KPC-Hes1-KO' (negatively correlated)
Rank in Ordered Dataset
Enrichment profile
Hits
Ranking metric scores

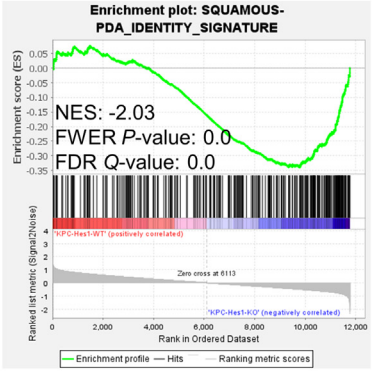
Enrichment plot: SQUAMOUS-
PDA_IDENTITY_SIGNATURE
NES: -2.03
FWER P-value: 0.0
FDR Q-value: 0.0
Enrichment score (ES)
Ranked list metric (Signal2Noise)
'KPC-Hes1-WT' (positively correlated)
Zero cross at 6113
'KPC-Hes1-KO' (negatively correlated)
Rank in Ordered Dataset
Enrichment profile
Hits
Ranking metric scores

D

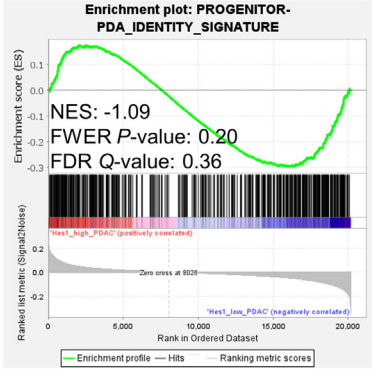
Enrichment plot: PROGENITOR-
PDA_IDENTITY_SIGNATURE
NES: -1.09
FWER P-value: 0.20
FDR Q-value: 0.36
Enrichment score (ES)
Ranked list metric (Signal2Noise)
'Hes1_high_PDAC' (positively correlated)
Zero cross at 8026
'Hes1_low_PDAC' (negatively correlated)
Rank in Ordered Dataset
Enrichment profile
Hits
Ranking metric scores

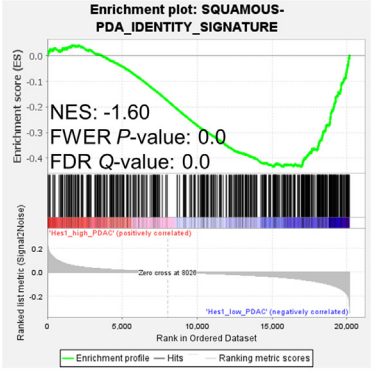
Enrichment plot: SQUAMOUS-
PDA_IDENTITY_SIGNATURE
NES: -1.60
FWER P-value: 0.0
FDR Q-value: 0.0
Enrichment score (ES)
Ranked list metric (Signal2Noise)
'Hes1_high_PDAC' (positively correlated)
Zero cross at 8026
'Hes1_low_PDAC' (negatively correlated)
Rank in Ordered Dataset
Enrichment profile
Hits
Ranking metric scores

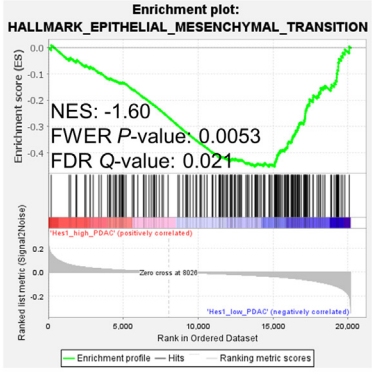
Enrichment plot:
HALLMARK_EPITHELIAL_MESENCHYMAL_TRANSITION
NES: -1.60
FWER P-value: 0.0053
FDR Q-value: 0.021
Enrichment score (ES)
Ranked list metric (Signal2Noise)
'Hes1_high_PDAC' (positively correlated)
Zero cross at 8026
'Hes1_low_PDAC' (negatively correlated)
Rank in Ordered Dataset
Enrichment profile
Hits
Ranking metric scores

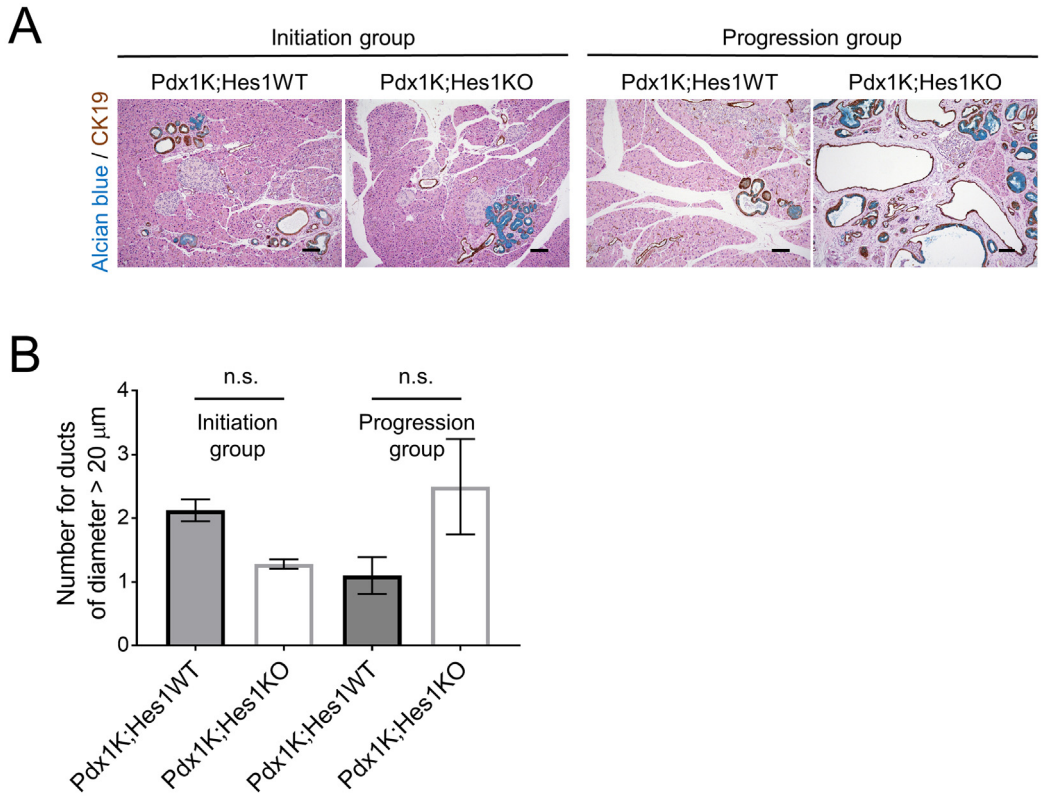


**Supplementary Figure 9.** (*A*) Alcian blue staining and IHC for CK19 in the pancreas of Pdx1K;Hes1KO and Pdx1K;Hes1WT mice. *Scale bar*, 100 $\mu$m. (*B*) Comparison of the number of ducts with diameter >20 $\mu$m between Pdx1K;Hes1KO and Pdx1K;Hes1WT mice in the initiation and progression groups. Diameter of pancreatic ducts in CK19-positive and Alcian blue-negative area was manually measured. Plotted values represent the mean ± standard deviation. n.s.; not significant.

**Supplementary Figure 8.** (*A*) Gene set enrichment analysis (GSEA) revealing the significant upregulation of gene sets in Hes1KO PDAC cells compared with that in Hes1WT PDAC cells. GOBP, Gene Ontology Biological Process. (*B*) Gene ontology analysis of upregulated genes in Hes1KO PDAC cells. Subtype analysis of mice (*C*) PDAC and (*D*) human PDAC via GSEA. (*D*) GSEA reveals the significant upregulation of epithelial-mesenchymal transition–related genes in Hes1-low PDAC. FDR, false discovery rate; FWER, family-wise error rate; NES, normalized enrichment score.

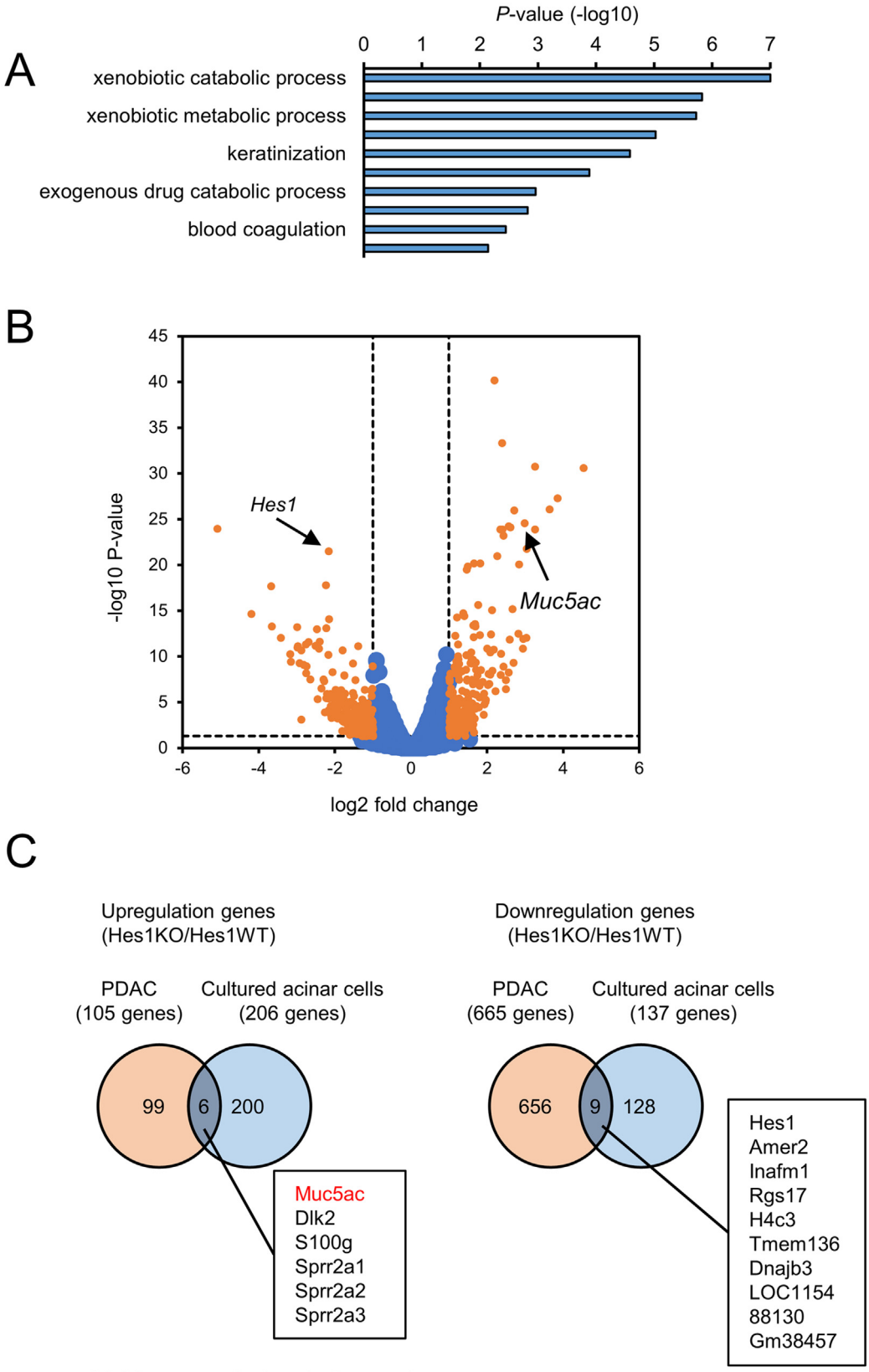


PDAC, pancreatic ductal adenocarcinoma

**Supplementary Figure 10.** (*A*) Gene ontology analysis of upregulated genes in Hes1KO cultured acinar cells compared with Hes1WT acinar cells. (*B*) Volcano plot of the differentially expressed genes between Hes1KO and Hes1WT in cultured acinar cells. Significantly down-regulated or up-regulated genes are indicated in *orange*, whereas those with no significant changes are indicated in *blue*. The *black vertical dashed lines* highlight $\log_2$ fold changes of $-1$ and 1, whereas the *black horizontal dashed line* represents a *P* value of .05. (*C*) Venn diagram of the differentially expressed genes in PDAC and cultured acinar cells by *Hes1* KO (up-regulated [*left*] and down-regulated genes [*right*] by *Hes1* KO). The number in each *circle* represents the number of genes ($|\log_2$ fold change$| \geq 1$; $P \leq .05$).